the mutant Müllerian duct was round and piled up, compared with the tapered form in control mice, as shown by *in situ* hybridization of *Lhx1* (Fig. 3D). This observation is reminiscent of Müllerian duct-specific *Lhx1* mutant mice, which show impaired migratory activity in the tip regions (Huang *et al.*, 2014). However, our mutant mice retained *Lhx1* expression, which was confirmed by section immunostaining (Fig. 5 A,C), as well as by *in situ* hybridization as shown in Fig. 3D. The unaltered *Lhx1* expression observed in both ducts of the mutant mice indicates that loss of *Lhx1* expression is not the major cause of the Müllerian duct defects.

Canonical Wnt signaling is not affected in the mutant Müllerian duct tips

Wnt9b is expressed in the Wolffian duct and its deletion results in absence of the Müllerian duct (Carroll *et al.*, 2005). This process of Müllerian duct formation, as well as tubule formation in the kidney, is considered to be mediated by the mesenchymal-to-epithelial transition evoked by the β-catenin/Lef1-dependent canonical Wnt pathway. Indeed, Lef1 staining was detected in epithelia of the control Müllerian duct tip regions, but not those of the Wolffian duct (Fig. 5B, C, left panel), suggesting that only the Müllerian duct epithelia respond to Wnt stimuli at this elongation stage. Despite the partial ablation of the Wolffian duct, the remaining duct expressed *Wnt9b* (Fig. 3A, B), and Lef1 expression in the mutant Müllerian duct tip was not reduced (Fig. 5B, right panel, n=4). Therefore, the canonical Wnt signaling evoked by Wnt9b and other possible ligands is unlikely to explain the elongation defects of the Müllerian duct in the mutant mice.

We also analyzed phosphorylated Smad1/5/8 (pSmad1/5/8), a downstream effector of Bmp signaling. However, we did not detect any signals in control mice, and no increased staining was observed in mutant mice (Fig. 5 D,E). Therefore, currently unidentified mechanisms could exist to explain the Müllerian elongation defects upon Wolffian duct truncation.

Discussion

We genetically ablated the Wolffian duct and demonstrated that the preformed Wolffian duct is required for proper Müllerian duct elongation. Although *Lhx1* is required for this process in both cell-autonomous and non-cell-autonomous manners, *Lhx1* expression in the mutant mice was not impaired. We also ruled out major extracellular signals, such as Wnt and Bmp, meaning that the Wolffian duct may regulate Müllerian duct elongation by currently unidentified mechanisms.

It is generally considered that the duct tip tends to possess mesenchyme-like characteristics with high migration ability, while the stalk region forms a tight layer of epithelia by a similar mechanism to the mesenchymal-to-epithelial transition. Canonical Wnt activity often enhances the static nature of the epithelia, while the non-canonical pathway promotes cell migration. According to the GUDMAP database (Little *et al.*, 2007), many Wnt ligands, as well as the frizzled (fz) receptors, are expressed in both the Müllerian and Wolffian ducts during mid-gestation. These ligands include Wnt5a, Wnt7b, and Wnt9b in the Wolffian duct, and Wnt4, Wnt5a, Wnt7a, and Wnt7b in the Müllerian duct (http://www.gudmap.org/). Our data showing exclusive Lef1 staining in the Müllerian duct epithelia in both the control and mutant embryos suggest that only the Müllerian duct responds to these ligands and that the canonical Wnt pathway is unlikely to explain the phenotype of the mutant mice. However, it is still possible that the non-canonical Wnt pathway plays a role in tip migration. At present, active forms of small GTPases (Rho, Rac, or Cdc42) involved in the non-canonical pathway and migration can only be measured by biochemical approaches that require large numbers of cells. Considering the very small size of the Müllerian duct tip, reagents or techniques that can detect the non-canonical activity should be developed to unequivocally determine whether the non-canonical pathway is responsible for the mutant phenotype.

Shh is expressed in the Wolffian duct, and could be one of the candidate molecules that we have not tested. However, Wolffian duct-specific deletion of *Shh* has no effects on Müllerian duct elongation (Murashima *et al.*, 2014). Other possibilities include cell-cell contacts, instead of soluble factors, considering the close proximity between the Müllerian and Wolffian ducts. Indeed, a role of fibronectin in Wolffian duct formation was reported in chick embryos (Yoshino *et al.*, 2014). According to the GUDMAP database, integrin β7 is expressed in the Müllerian duct, while nephronectin is expressed in the Wolffian duct. Given the importance of nephronectin in the interactions between the metanephric mesenchyme and the Wolffian duct-derived ureteric bud (Linton *et al.*, 2007), it may be worth examining the roles of this type of adhesion molecule in Müllerian duct elongation. However, the currently available datasets have used entire ducts that are anatomically dissected. Identification of markers for the Müllerian duct tip and subsequent generation of GFP-knockin mice, followed by microarray analyses, will help to elucidate the detailed mechanisms of Müllerian duct elongation. Although the precise mechanisms remain to be solved, our mouse model will serve as a useful tool to analyze the interaction between these two reproductive systems.

It was reported that a subset of human patients with uterus hypoplasia display kidney hypoplasia (Oppelt *et al.*, 2007; Woolf and Allen, 1953). At least some of these cases may be derived from primary defects in the Wolffian duct, which affects the Müllerian duct in a non-cell-autonomous manner, similar to the mouse model described in this paper. Thus, any genes that cause developmental arrest of the Wolffian duct may lead to malformation of the uterus and kidney. Alternatively, several genes, including *Lhx1*, are shared for the development of both the Wolffian and Müllerian ducts, and therefore mutations in one particular gene could impair the formation of both organs. Emerging exome sequencing techniques will help to identify the responsible genes in human diseases, which will further accelerate our understanding of the formation of these two reproductive duct systems.

Materials and Methods

Generation of mutant mice

Hoxb7Cre, *R26-GFP-DTA*, and *R26-tdTomato* mice were obtained from the Jackson Laboratory (Ivanova *et al.*, 2005; Madisen *et al.*, 2010; Yu *et al.*, 2002). The primers used for genotyping were as follows: Cre1 (5′-AGGTTCGTTCACTCATGGA-3′) and Cre2 (5′-TCGACCAGTTTAGTTACCC-3′) for the Cre allele (250-bp product); DTA-mt (5′-GCGAAGAGTTTGTCCTCAACC-3′), DTA-F (5′-AAAGTCGCTCTGAGTTGTTAT-3′), and DTA-R (5′-GGAGCGGGAGAAATGGATATG-3′) for the *R26R-GFP-DTA* allele (wild-type: 600-bp product; mutant: 340-bp product); Tomato-1 (5′-AAGGGAGCTGCAGTGAGTA-3′), Tomato-2 (5′-CCGAAAATCTGTGGGAAGTC-3′), Tomato-3 (5′-GGCATTAAAGCAGCGTATCC-3′), and Tomato-4 (5′-CTGTTCCTGTACGGCATGG-3′) for the *R26-tdTomato*

allele (wild-type: 297-bp product; mutant: 196-bp product). The sex of the embryos was determined by detection of the male-specific *Sry* allele (220 bp product) using the following primers: Sry-Fw6 (5′-TGACTGGGATG-CAGTAGTTC-3′), and Sry-Rev6 (5′-TGTGCTAGAGAGAAACCCTG-3′). The PCR amplifications were performed under identical conditions using GoTaq DNA polymerase (Promega). The procedure involved denaturation at 95°C for 5 min, followed by 35 cycles of 95°C for 30 s, 58°C for 60 s, and 72°C for 30 s, and a final extension at 72°C for 7 min. The PCR products were analyzed by electrophoresis in a 1.2% agarose gel and visualized by ethidium bromide staining. All animal experiments were performed in accordance with institutional guidelines and ethical review committees.

Whole-mount* in situ *hybridization

Dissected reproductive organs were fixed with 4% paraformaldehyde and subsequently with methanol. Rehydrated samples were treated with proteinase K (10 μg/ml) for 1 h at room temperature, followed by post-fixation with 2 mg/ml glycine for 30 s and then 0.2% glutaraldehyde/4% paraformaldehyde for 20 min. Subsequently, the samples were processed using an automated InsituPro VS (Intavis AG) according to the manufacturer's protocol. The template for the *Lhx1* probe was kindly provided by Dr. R. Behringer. The *Wnt9b* probe was generated as described (Uchiyama *et al.*, 2010).

Immunohistochemical analysis

Histological examinations were performed as described previously (Kanda *et al.*, 2014). Mice were fixed in 10% formalin, embedded in paraffin, and cut into 6-μm sections. The Müllerian duct tip was identified by serial horizontal sectioning, and sections within 90 μm from the tip were evaluated. Immunostaining was carried out automatically using a BlueMap kit and an automated Discovery System (Roche) or manually for immunofluorescence staining. The following primary antibodies were used: rabbit anti-Pax2 (Covance); mouse anti-Lhx1/2 (Developmental Studies Hybridoma Bank; Cat. No. 4F2); and rabbit anti-Lef1 (Cell Signaling). TdT-mediated dUTP nick end labeling (TUNEL) assays were performed using an ApopTag Plus Fluorescein *In situ* Apoptosis Detection Kit (Millipore), and the signals were enhanced with Alexa 594-conjugated streptavidin (Invitrogen). For proliferation analyses, embryos were harvested at 1 h after intraperitoneal BrdU administration (0.03 mg/g body weight). The signals were detected using an anti-BrdU antibody (BD Pharmingen) and an Alexa 594-conjugated secondary antibody. The percentages of BrdU- and TUNEL-positive cells in Müllerian duct epithelia were calculated using at least three pairs of control and mutant embryos (two different sections/embryo). The mean and standard deviation were calculated. Immunofluorescence was visualized with an LSM780 confocal microscope (Carl Zeiss).

Acknowledgments

We thank Y. Kaku, A. Taguchi, S. Fujimura, and M. Hoshi for helpful advice. This study was supported by KAKENHI (25670413), MEXT, Japan.

References

BISHOP-CALAME S (1966). Experimental study of the organogenesis of the urogenital system of the chicken embryo. *Arc Anat Microsc Morphol Exp* 55: 215–309.

CARROLL TJ, PARK JS, HAYASHI S, MAJUMDAR A, MCMAHON AP (2005). Wnt9b plays a central role in the regulation of mesenchymal to epithelial transitions underlying organogenesis of the mammalian urogenital system. *Dev Cell* 9: 283–292.

HUANG C-C, ORVIS GD, KWAN KM, BEHRINGER RR (2014). Lhx1 is required in Müllerian duct epithelium for uterine development. *Dev Biol* 389: 124–136.

IVANOVAA, SIGNORE M, CARON, GREENE NDE, COPPAJ, MARTINEZ-BARBERA JP (2005). *In vivo* genetic ablation by Cre-mediated expression of diphtheria toxin fragment A. *Genesis* 43: 129–135.

KANDA S, TANIGAWA S, OHMORI T, TAGUCHI A, KUDO K, SUZUKI Y, SATO Y, HINO S, SANDER M, PERANTONI AO, SUGANO S, NAKAO M, NISHINAKA-MURA R (2014). Sall1 maintains nephron progenitors and nascent nephrons by acting as both an activator and a repressor. *J Am Soc Nephrol* 25: 2584–2595.

KOBAYASHI A, BEHRINGER RR (2003). Developmental genetics of the female reproductive tract in mammals. *Nat Rev Genet* 4: 969–980.

KOBAYASHI A, KWAN K-M, CARROLL TJ, MCMAHON AP, MENDELSOHN CL, BEHRINGER RR (2005). Distinct and sequential tissue-specific activities of the LIM-class homeobox gene Lim1 for tubular morphogenesis during kidney development. *Development* 132: 2809–2823.

LINTON JM, MARTIN GR, REICHARDT LF (2007). The ECM protein nephronectin promotes kidney development via integrin alpha8beta1-mediated stimulation of Gdnf expression. *Development* 134: 2501–2509.

LITTLE MH, BRENNAN J, GEORGAS K, DAVIES JA, DAVIDSON DR, BALDOCK RA, BEVERDAM A, BERTRAM JF, CAPEL B, CHIU HS, *et al.*, (2007). A high-resolution anatomical ontology of the developing murine genitourinary tract. *Gene Expr Patterns* 7: 680–699.

MADISEN L, ZWINGMAN TA, SUNKIN SM, OH SW, ZARIWALA HA, GU H, NG LL, PALMITER RD, HAWRYLYCZ MJ, JONES AR, LEIN ES, ZENG H (2010). A robust and high-throughput Cre reporting and characterization system for the whole mouse brain. *Nat Neurosci* 13: 133–140.

MIYAMOTO N, YOSHIDA M, KURATANI S, MATSUO I, AIZAWA S (1997). Defects of urogenital development in mice lacking Emx2. *Development* 124: 1653–1664.

MURASHIMA A, AKITA H, OKAZAWA M, KISHIGAMI S, NAKAGATA N, NISHINAKA-MURA R, YAMADA G (2014). Midline-derived Shh regulates mesonephric tubule formation through the paraxial mesoderm. *Dev Biol* 386: 216–226.

NISHINAKAMURA R (2008). Stem cells in the embryonic kidney. *Kidney Int* 73: 913–917.

OPPELT P, VON HAVE M, PAULSEN M, STRISSEL PL, STRICK R, BRUCKER S, WALLWIENER D, BECKMANN MW (2007). Female genital malformations and their associated abnormalities. *Fertil Steril* 87: 335–342.

ORVIS GD, BEHRINGER RR (2007). Cellular mechanisms of Müllerian duct formation in the mouse. *Dev Biol* 306: 493–504.

SHAWLOT W, BEHRINGER RR (1995). Requirement for Lim1 in head-organizer function. *Nature* 374: 425–430.

TORRES M, GÓMEZ-PARDO E, DRESSLER GR, GRUSS P (1995). Pax-2 controls multiple steps of urogenital development. *Development* 121: 4057–4065.

UCHIYAMA Y, SAKAGUCHI M, TERABAYASHI T, INENAGA T, INOUE S, KOBAYASHI C, OSHIMA N, KIYONARI H, NAKAGATA N, SATO Y, SEKIGUCHI K, MIKI H, ARAKI E, FUJIMURA S, TANAKA SS, NISHINAKAMURA R (2010). Kif26b, a kinesin family gene, regulates adhesion of the embryonic kidney mesenchyme. *Proc Natl Acad Sci USA* 107: 9240–9245.

WOOLF RB, ALLEN WM (1953). Concomitant malformations; the frequent, simultaneous occurrence of congenital malformations of the reproductive and urinary tracts. *Obs Gynecol* 2: 236–265.

YOSHINO T, SAITO D, ATSUTA Y, UCHIYAMA C, UEDA S, SEKIGUCHI K, TAKAHASHI Y (2014). Interepithelial signaling with nephric duct is required for the formation of overlying coelomic epithelial cell sheet. *Proc Natl Acad Sci U S A* 111: 6660–6665.

YU J, CARROLL TJ, MCMAHON AP (2002). Sonic hedgehog regulates proliferation and differentiation of mesenchymal cells in the mouse metanephric kidney. *Development* 129: 5301–5312.

Further Related Reading, published previously in the *Int. J. Dev. Biol.*

Induction of intermediate mesoderm by retinoic acid receptor signaling from differentiating mouse embryonic stem cells
Shiho Oeda, Yohei Hayashi, Techuan Chan, Minoru Takasato, Yuko Aihara,Koji Okabayashi, Kiyoshi Ohnuma and Makoto Asashima
Int. J. Dev. Biol. (2013) 57: 383-389
http://dx.doi.org/10.1387/ijdb.130058ma

Revisiting old vaginal topics: conversion of the Müllerian vagina and origin of the "sinus" vagina
Yi Cai
Int. J. Dev. Biol. (2009) 53: 925-934
http://dx.doi.org/10.1387/ijdb.082846yc

The developing female genital tract: from genetics to epigenetics
Julie Massé, Tanguy Watrin, Audrey Laurent, Stéphane Deschamps, Daniel Guerrier and Isabelle Pellerin
Int. J. Dev. Biol. (2009) 53: 411-424
http://dx.doi.org/10.1387/ijdb.082680jm

Charting the course of ovarian development in vertebrates
Kelly A Loffler and Peter Koopman
Int. J. Dev. Biol. (2002) 46: 503-510
http://dx.doi.org/10.1387/ijdb.12141437

Germ cells, gonads and sex reversal in marsupials
M B Renfree and G Shaw
Int. J. Dev. Biol. (2001) 45: 557-567
http://dx.doi.org/10.1387/ijdb.11417899

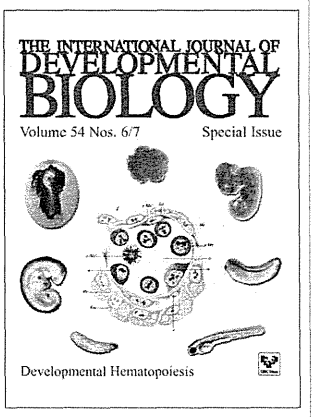

5 yr ISI Impact Factor (2013) = 2.879

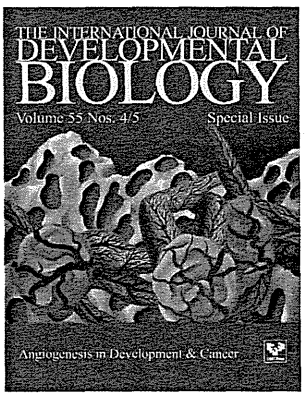

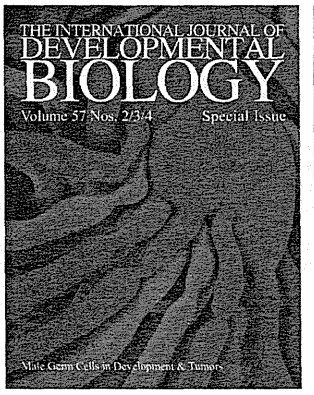

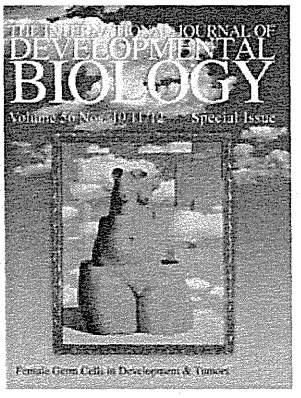

G Model
YDLD-2855; No. of Pages 7
ARTICLE IN PRESS

Digestive and Liver Disease xxx (2015) xxx–xxx

Contents lists available at ScienceDirect

Digestive and Liver Disease

journal homepage: www.elsevier.com/locate/dld

Liver, Pancreas and Biliary Tract

Relationship between 18-F-fluoro-deoxy-D-glucose uptake and expression of glucose transporter 1 and pyruvate kinase M2 in intrahepatic cholangiocarcinoma

Hideki Suzuki[a,*], Mina Komuta[b], Altan Bolog[a], Takehiko Yokobori[a], Satoshi Wada[a], Kenichiro Araki[a], Norio Kubo[a], Akira Watanabe[a], Mariko Tsukagoshi[a], Hiroyuki Kuwano[a]

[a] Department of General Surgical Science (Surgery I), Graduate School of Medicine, Gunma University, Japan
[b] Pathology Service, Saint-Luc University, Belgium

ARTICLE INFO

Article history:
Received 30 September 2014
Accepted 17 March 2015
Available online xxx

Keywords:
18F-2-fluoro-2-deoxy-D-glucose-positron emission tomography
Glucose transporter 1
Glycolytic metabolism
Intrahepatic cholangiocarcinoma
Pyruvate kinase type M2

ABSTRACT

Background: Cholangiocellular carcinoma is characterized by elevated glucose consumption, resulting in an increased uptake of 18F-2-fluoro-2-deoxy-D-glucose (18F-FDG). This study investigates the relationship between 18F-FDG uptake and tumour glucose metabolism.
Methods: This was a retrospective analysis of 19 patients with cholangiocellular carcinoma. Immunohistochemistry for glucose transporter 1 and pyruvate kinase type M2 were performed. Overall tumour glucose metabolism was evaluated by measuring 18F-FDG uptake and the protein expression levels of glucose transporter 1 and pyruvate kinase type M2.
Results: 18F-FDG uptake had a strong positive correlation with histological differentiation. Both tumour status ($p = 0.044$) and tumour size ($p = 0.011$) were correlated with primary tumour 18F-FDG uptake. Glucose transporter 1 expression correlated with histological differentiation ($p = 0.017$), while pyruvate kinase type M2 expression tended to correlate with lymph node metastasis ($p = 0.051$). Glucose transporter 1 expression was strongly related to the standard uptake value ($p = 0.001$), but that of pyruvate kinase type M2 was not ($p = 0.461$).
Conclusions: Glucose transporter 1 expression exhibits a strong correlation with 18F-FDG uptake in cholangiocellular carcinoma tissue, while pyruvate kinase type M2 expression was not associated with fluoro-2-deoxy-D-glucose uptake. In addition to its glycolytic function, pyruvate kinase type M2 has a variety of roles and its expression may enhance tumour cell invasion and promote the lymph node metastasis of intrahepatic cholangiocarcinoma.

1. Introduction

Intrahepatic cholangiocarcinoma (ICC) is the second most common primary hepatic malignancy worldwide. ICC originates from the neoplastic transformation of cholangiocytes into intrahepatic tumours and has a poor prognosis with restricted treatment alternatives. Surgical resection is the only definitive treatment strategy for cholangiocellular carcinoma (CCC); however, local recurrence and metastasis are very common, and the 5-year survival rate is extremely low [1–4]. Previous studies attempted to identify useful prognostic factors, with some authors claiming that lymph node involvement is indicative of outcome [5–7]. Therefore, accurate staging including lymph node metastasis is essential for appropriate patient management [8].

As cancer cell growth is heavily dependent on glucose metabolism, the underlying pathways could have a considerable effect on the prognosis of patients with CCC. Glycolytic metabolism lies at the centre of cancer biology, thus, understanding the relationship between the 18F-fluorodeoxyglucose (FDG) uptake and glucose transporter 1 (Glut-1) and pyruvate kinase M2 (PKM2) expression is important. Positron emission tomography (PET) with 18F-FDG provides metabolic information and has been widely used for cancer diagnosis, staging, and detection of recurrence. 18F-FDG is transported into tumour cells by glucose transporter proteins

* Corresponding author at: Department of General Surgical Science (Surgery I), Graduate School of Medicine, Gunma University, 3-39-22 Showa-machi, Maebashi 371-8511, Japan. Tel.: +81 272 20 8224; fax: +81 272 20 8230.
E-mail address: hidesuzuki044@gmail.com (H. Suzuki).

http://dx.doi.org/10.1016/j.dld.2015.03.017
1590-8658/

Please cite this article in press as: Suzuki H, et al. Relationship between 18-F-fluoro-deoxy-D-glucose uptake and expression of glucose transporter 1 and pyruvate kinase M2 in intrahepatic cholangiocarcinoma. Dig Liver Dis (2015), http://dx.doi.org/10.1016/j.dld.2015.03.017

present on the cell membrane; intracellularly, it is phosphorylated by hexokinase to FDG-6-phosphate, a highly polar molecule that cannot diffuse out of the cell. FDG-6-phosphate within the cancer tissue can then be visualized by PET. Measuring the increased 18F-FDG uptake on PET scans has been used in diagnostic imaging of patients with CCC. Cancer cell growth is heavily dependent on glucose metabolism as its major energy source and, as a result, the 18F-FDG uptake pattern on PET may be an indicator of tumour growth and prognosis [9–12]. Investigations of liver tumours have shown that FDG-PET is useful for tumour characterization as well as assessing therapeutic responses and outcomes [13,14]. However, 18F-FDG uptake patterns are variable in patients with ICC.

18F-FDG uptake by tumour cells largely depends on the presence of facilitated glucose transporters, and glucose metabolism is regulated by the glucose uptake induced by these transporters. Among the mechanisms that contribute to the glycolytic phenotype, glucose transporter 1 (Glut-1) overexpression has been reported for a large variety of tumours [15–17]. As an example, Glut-1 expression is significantly correlated with 18F-FDG uptake in patients with CCC [18]. In patients with colorectal or gastric carcinoma, Glut-1 overexpression was associated with tumour aggressiveness and poor survival [19].

Most cancer cells primarily metabolize glucose by glycolysis even in the presence of ample oxygen, whereas most normal cells completely catabolize glucose via oxidative phosphorylation. In other words, tumour cells convert large amounts of glucose to lactate, even in the presence of oxygen. This unique aspect of tumour metabolism is called aerobic glycolysis or the Warburg effect [20,21]. Recent studies have shown that this effect is regulated by the key glycolytic enzyme, PKM2 [22]. In addition to its glycolytic functions, PKM2 can be translocated into the nucleus, where it activates the transcription of various genes by interacting with, and phosphorylating, specific nuclear proteins [23]. Yang et al. reported that the endothelial growth factor receptor (EGFR) induces PKM2 nuclear translocation and stimulates PKM2's involvement in gene transcription regulation [24]. This suggests that the protein kinase activity of PKM2 may play a pivotal role in controlling cell proliferation.

In the present study, we sought to identify factors associated with patient outcome after surgical management of ICC. We also examined the association between 18F-FDG uptake and the expression of Glut-1 and PKM2 with a focus on cancer cell glucose metabolism.

2. Materials and methods

2.1. Patients

We performed a retrospective study of ICC patients who underwent curative surgery from April 2002 to December 2012 at the Department of General Surgical Science, Graduate School of Medicine, Gunma University, Japan. Patients who did not undergo preoperative 18F-FDG imaging were excluded. ICC was defined as adenocarcinoma arising from the second order or more distal branches of intrahepatic bile ducts, and all ICCs were pathologically confirmed. ICCs were further classified into two groups based on their possible cell of origin: mucin-producing with CC features (muc-ICC), and focal hepatocytic differentiation with ductular areas (mixed-ICC) [25]. Before liver resection, all patients underwent liver function tests and cancer antigen 19-9 (CA 19-9) assays. Preoperative evaluation was carried out with ultrasonography (US), computed tomography (CT), magnetic resonance imaging (MRI), and FDG-PET. In addition, some patients underwent endoscope retrograde cholangio-pancreatography (ERCP) and/or percutaneous transhepatic biliary drainage (PTCD) for diagnosis and/or biliary decompression. ICC was classified into three categories according to the macroscopic typing proposed by the Liver Cancer Study Group of Japan [26]: mass-forming (MF), periductal-infiltrating (PI), or intraductal-growth (IG). When more than one type was found, the predominant type was recorded.

Contraindication for surgery was determined as follows: (1) distant metastasis, (2) peritoneal dissemination, (3) multiple para-aortic lymph node metastases, (4) extensive vascular involvement and/or multiple intrahepatic metastases, or (5) severe liver cirrhosis. Suspected regional lymph node metastasis on CT and/or MRI was not a contraindication for surgery. Curative resection was defined as total excision of the entire tumour including the primary tumour and associated lymph node. Staging was performed according to the pTNM classification of the International Union Against Cancer [27].

Standard demographic and clinicopathological data were collected, including age, gender, and primary tumour characteristics. Also, tumour-related data were collected, including tumour location, size, number, macroscopic type, pathological tumour staging, lymph node metastases, tumour differentiation, and surgical margin status. Data on treatment-related variables, such as type of surgery, resection of extrahepatic bile duct, operation time, and blood loss, were also recorded.

2.2. FDG-PET study

The detailed methods for PET scanning in our institution have been previously described [28]. Briefly, the PET study was carried out using a Discovery STE (GE Healthcare, Waukesha, WI, USA) and Biograph 16 (Siemens Medical Solutions, Malvern, PA, USA) scanners, with a 700-mm field of view (FOV) and slice thickness of 3.27 mm. Prior to FDG-PET scanning, patients fasted for at least 6 h, and 200–250 megabecquerel (MBq) 18F-FDG were injected intravenously. Whole-body PET-CT images were obtained 60 min after 18-FDG administration. The emission scan started from the skull base and continued to the upper thigh in 2-dimensional mode 50–60 min after the injection. The PET scans were compared with the corresponding CT images for accurate tumour localization. The coronal, sagittal, and axial images of the patients were qualitatively evaluated to determine whether tumour 18F-FDG uptake was higher than that in the surrounding non-cancerous hepatic tissue. The standardized uptake value (SUV) was defined as the concentration of radioactivity in the tissue or lesion (MBq/g) × patient body weight (g)/injected dose (MBq).

2.3. Immunohistochemistry

The resected surgical specimens were fixed with 10% formaldehyde, embedded in paraffin blocks, cut into 4-μm-thick sections, and mounted on glass slides. The staining procedure was performed using standard streptavidin-biotin peroxidase complex (S-ABC) methods. All sections were incubated at 60 °C for 60 min, deparaffinized in xylene, rehydrated, and incubated with fresh 0.3% hydrogen peroxide in 100% methanol for 30 min at room temperature to block endogenous peroxidase activity. After rehydration through a graded series of the ethanol treatments, antigen retrieval was carried out in 10 mM citrate buffer (pH 6.4) at 98–100 °C for 20 min, and sections were passively cooled to 30 °C. After rinsing the section in 0.1 M phosphate-buffered saline (PBS, pH 7.4), nonspecific binding sites were blocked by incubation with 10% normal rabbit or goat serum for 30 min. The sections were incubated with a rabbit anti-PKM2 polyclonal antibody (Signalway Antibody, College Park, MD, USA) at a 1:200 dilution, and Glut-1 (AB15309; Abcam, Cambridge, UK) at a 1:400 dilution in PBS containing 1%

Please cite this article in press as: Suzuki H, et al. Relationship between 18-F-fluoro-deoxy-D-glucose uptake and expression of glucose transporter 1 and pyruvate kinase M2 in intrahepatic cholangiocarcinoma. Dig Liver Dis (2015), http://dx.doi.org/10.1016/j.dld.2015.03.017

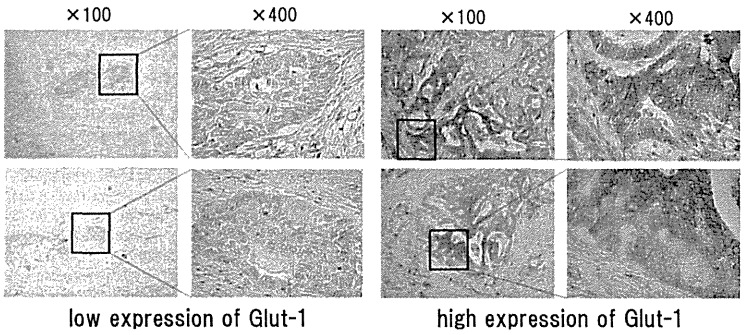

Fig. 1. Immunohistochemistry for glucose transporter 1 in cholangiocellular carcinoma. Glucose transporter 1 expression in representative areas of tumours in the negative and the positive. Sections were immunolabeled using a glucose transporter 1 antibody and an avidin-biotin technique. Magnification ×400.

bovine serum albumin overnight at 4 °C, and then at room temperature for 30 min. The sections were washed in PBS, incubated with biotinylated anti-rabbit IgG, A, and M solution (Nichirei Co., Tokyo, Japan) for 30 min at room temperature, and finally incubated in a streptavidin–biotin peroxidase complex solution (Nichirei Co.) for 30 min. The chromogen 3, 3′-diaminobenzidine tetrahydrochloride was applied as a 0.02% solution containing 0.005% hydrogen peroxide in a 50 mM ammonium acetate–citrate acid buffer (pH 6.0). The sections were lightly counterstained in Mayer's haematoxylin and mounted.

Intravascular red cells, which stained strongly in all tissue sections, served as internal controls. Glut-1 immunoreactivity was cytoplasmically localized in cancer cells, and the staining intensity and number of positive cells were scored for each specimen. The percentage of Glut-1-positive cells was rated using a semi-quantitative scale as 0–10% or 11–100%, considered as low or high expression, respectively (Fig. 1).

The proportion of tumour cells was classified as follows based on staining intensity: 0–25% (low expression) or >25% (high expression) of PKM2-positive tumour cells (Fig. 2). The epithelial membrane antigen (EMA, MUC1) was used to classify Muc-ICC and Mixed-ICC according to what reported in a previous publication [25].

2.4. Statistical methods

Statistical computations were performed with the JMP software (SAS Institute, Cary, NC, USA). Continuous variables are expressed as medians and were compared using the Wilcoxon test, whereas categorical variables were compared using the Fisher's exact or chi-square test. The Kaplan–Meier method was used to analyse overall survival, and the log-rank test was used to assess differences in survival. Statistical significance was defined as $p < 0.05$. For disease-specific survival, only deaths attributable to recurrent cancer were considered as events. Patients who died from secondary causes without recurrence were censored.

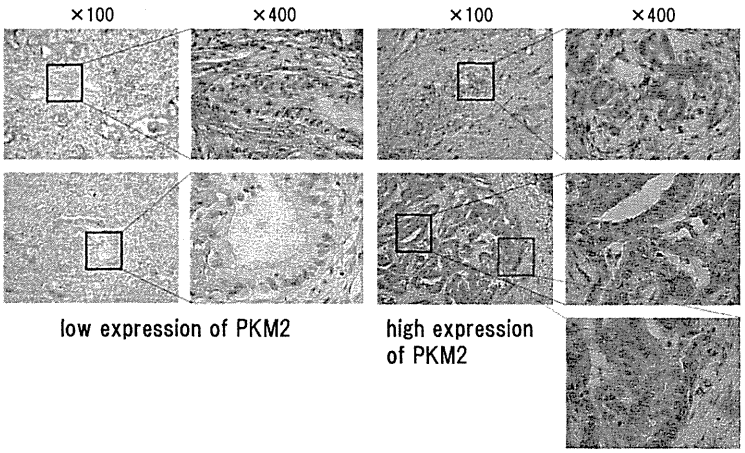

Fig. 2. Immunohistochemistry for pyruvate kinase M2. Low and high pyruvate kinase M2 expression in representative areas of tumour tissue. Tumours with more than 25% pyruvate kinase M2-positive cells were considered positive, and those with less than 25% pyruvate kinase M2-positive cells were considered negative. Glut-1, glucose transporter 1.

Please cite this article in press as: Suzuki H, et al. Relationship between 18-F-fluoro-deoxy-D-glucose uptake and expression of glucose transporter 1 and pyruvate kinase M2 in intrahepatic cholangiocarcinoma. Dig Liver Dis (2015), http://dx.doi.org/10.1016/j.dld.2015.03.017

Table 1
Patient demographics, clinicopathologic characteristics and surgical results.

Characteristics	No. of patients (%)	p
Age (years)		0.354
<70/≥70	7 (36.8)/12 (63.2)	
Gender		0.759
Male/female	12 (63.2)/7 (36.8)	
Location		0.069
Right/left	9 (47.4)/10 (52.6)	
CA 19-9 (U/ml)		0.036
<37/>37	10 (52.6)/9 (47.4)	
Macroscopic tumour growth type		0.921
IG/MF/PI	3 (15.8)/11 (57.9)/5 (26.3)	
Histological classification		0.147
Muc-ICC/Mixed-ICC	12 (63.2)/7 (36.8)	
Maximum diameter (mm)		0.421
<40/≥40	11 (57.9)/8 (42.1)	
Histologic grading		0.135
Well or moderate/poor	13 (68.4)/6 (31.6)	
T stage (TNM)		0.026
T1, T2/T3, T4	8 (42.1)/11 (57.9)	
Lymph node metastasis		0.453
Absent/present	12 (63.2)/7 (36.8)	
Stage		0.299
I, II/III, IV	8 (42.1)/11 (57.9)	
SUV		0.301
<4/>4	10 (52.6)/9 (47.4)	
Lobectomy		0.007
Done/none	14 (73.7)/5 (26.3)	
Resection of extrahepatic bile duct		0.114
Done/none	3 (15.8)/16 (84.2)	
Radicality		0.017
R0/R+	6 (31.6)/13 (68.4)	
Operation time (min)		0.907
<370/≥370	8 (42.1)/11 (57.9)	
Blood loss (ml)		0.090
<1350/≥1350	11 (57.9)/8 (42.1)	

CA19-9: carbohydrate antigen 19-9, IG: intraductal growth type, MF: mass-forming type, PI: periductal infiltrating type, Muc-ICC: mucin producing ICC, Mixed-ICC: ICC with mixed features, ICC: intrahepatic cholangiocarcinoma SUV: standardized uptake value

3. Results

Patient demographics and surgical results are shown in Table 1. The 19 patients who underwent surgical resection with curative intent were 12 males and 7 females with a median age of 70 years (range 57–80 years). The CA19-9 levels were elevated in 9 patients (47%). With regard to the macroscopic findings of the excised tumour, 11 (57.9%), 5 (26.3%), and 3 (15.8%) were MF, PI, and IG type, respectively. The median tumour size was 4.8 cm (range 2.8–8.5 cm). Histological examination revealed poorly differentiated carcinoma in 6 cases (31.6%), and well-differentiated or moderately differentiated carcinoma in 13 cases (68.4%). Based on the cell-of-origin classification, 12 ICCs were diagnosed as Muc-ICCs (63.1%), and 7 were Mixed-ICCs (36.8%). Among the 19 cases, 7 had affected lymph nodes (36.8%). More than half of the patients (57.9%) were diagnosed with advanced stage III or IV cancer. With regard to preoperative FDG-PET scanning, the detection rate for ICC was 89.4% (17/19), and the mean tumour SUV was 6.0 (range 1.5–14.5). A lobectomy was performed in 14 cases (73.7%), and curative resection was achieved in 7 patients (26.3%). Extrahepatic bile duct resection was performed in 3 patients (15.8%). Major lobectomy significantly improved the 3-year overall survival (51.4% vs. 0%; $p = 0.007$). When R0 resections were compared with R1/R2 resections, curative resection also significantly improved the 3-year overall survival (83.3% vs. 18.3%, $p = 0.017$; data not shown). The patients with muc-ICC tended to have poorer prognoses compared to those with mixed-ICC.

Table 2
Relationship between clinicopthological characteristics and standardized uptake values of intrahepatic cholangiocarcinoma.

Factors	Standardized uptake value (n)	P
Macroscopic type		0.182
PI/IG	4.5 ± 1.5 (8)	
MF	7.2 ± 1.2 (11)	
Histological classification		0.486
Muc-ICC	6.6 ± 1.2 (12)	
Mixed-ICC	5.1 ± 1.6 (7)	
CA19-9 (U/ml)		0.930
<37	6.1 ± 1.5 (9)	
>37	5.9 ± 1.4 (10)	
Histological differentiation		0.004
Well/moderate	4.3 ± 0.9 (13)	
Poor	9.8 ± 1.4 (6)	
Tumour status		0.026
T1, T2	4.2 ± 1.4 (8)	
T3, T4	7.4 ± 1.2 (11)	
Tumour size		0.011
<4 cm	4.0 ± 1.1 (11)	
>4 cm	8.8 ± 13 (8)	
Lymph-node metastasis		0.242
Absent	5.3 ± 1.2 (13)	
Present	7.6 ± 1.6 (7)	
Tumour grade		0.779
I, II	6.4 ± 1.5 (8)	
III, IV	5.8 ± 1.3 (11)	
Radicality		0.156
R0	4.0 ± 1.7 (6)	
R+	6.9 ± 1.1 (13)	

IG, intraductal growth type, MF, mass-forming type, PI, periductal infiltrating type, Muc-ICC, mucin producing ICC, Mixed-ICC, ICC with mixed features, ICC, intrahepatic cholangiocarcinoma, CA19-9, carbohydrate antigen 19-9.

3.1. Relationship between clinicopathological data and SUV in ICC

The two criteria for correct detection by PET/CT are positive FDG uptake and correct anatomical location of the tumour. ICC was detected in 17/19 patients by PET/CT and 15/19 patients by CT. As shown in Table 2, there was no significant relationship between tumour SUV and macroscopic type, histological classification, CA19-9 level, lymph node metastasis, tumour grade, or curability. However, primary tumour SUV was inversely correlated with histological differentiation ($p = 0.004$). Moreover, both tumour status ($p = 0.026$) and size ($p = 0.011$) were also correlated with primary tumour FDG uptake.

3.2. Correlations between Glut-1 expression and clinicopathological factors

We examined Glut-1 expression in representative negative and positive tumour areas. Sections were immunolabeled with a glucose 1 antibody using the avidin-biotin technique. Glut-1 immunolabeling was positive in 13 (68.4%) of the 19 primary lesions. Table 3 shows the comparative analysis between Glut-1 immunohistochemical findings and clinicopathological characteristics. Glut-1 expression was correlated with histological differentiation ($p = 0.017$), but there were no significant relationships between Glut-1 expression and other clinicopathological characteristics including maximum diameter, lymph node metastasis, and stage. However, 83% (10/13) of muc-ICCs had positive Glut-1 expression, suggesting a possible association between muc-ICC and Glut-1 expression.

3.3. Correlations between PKM2 expression and clinicopathological factors

The PKM2 protein was detected in 11 cases (57.9%). As shown in Fig. 2, PKM2 was mainly localized in the cytoplasm of primary

Please cite this article in press as: Suzuki H, et al. Relationship between 18-F-fluoro-deoxy-D-glucose uptake and expression of glucose transporter 1 and pyruvate kinase M2 in intrahepatic cholangiocarcinoma. Dig Liver Dis (2015), http://dx.doi.org/10.1016/j.dld.2015.03.017

Table 3
Correlations between glucose transporter 1 expression, pyruvate kinase type m2 expression and clinicopathological factors.

Characteristics (%)	Glut 1 expression		*P* value	PKM2 expression		*P* value
	Negative (n = 6)	Positive (n = 13)		Negative (n = 8)	Positive (n = 11)	
Age (years)			0.829			0.960
<70 (36.8)/≥70 (63.2)	2/4	5/8		3/5	4/7	
Gender			0.138			0.960
Male (63.2)/female (36.8)	5/1	7/6		5/3	7/4	
CA19-9 (U/ml)			0.402			0.258
<37 (52.6)/≥37 (47.4)	4/2	6/7		3/5	7/4	
Histological classification			0.068			0.360
Muc-ICC (63.2)/Mixed-ICC (47.4)	2/4	10/3		5/3	7/4	
Maximum diameter			0.113			0.552
<40 (57.9)/≥40 (42.1)	5/1	6/7		4/4	7/4	
Histologic grading			0.017			0.113
Well or moderate (68.4)/poor (31.6)	6/0	7/6		7/1	6/5	
T stage (TNM)			0.140			0.728
T1, T2 (42.1)/T3, T4 (57.9)	4/2	4/9		3/5	5/6	
Lymph node metastasis			0.198			0.051
Absent (63.2)/Present (36.8)	5/1	7/6		7/1	5/6	
Stage			0.596			0.728
I, II (42.1)/III, IV (57.9)	2/4	6/7		3/5	5/6	
SUV max			0.001			0.461
<4 (52,6)/>4 (47.4)	6/0	4/9		5/3	5/6	

Glut-1, glucose transporter 1, PKM2, pyruvate kinase type M2, CA19-9, carbohydrate antigen 19-9, Muc-ICC, mucin producing ICC, Mixed-ICC, ICC with mixed features, ICC, intrahepatic cholangiocarcinoma, SUV, standardized uptake value.

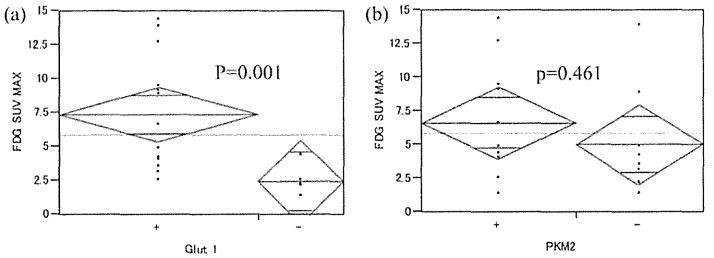

Fig. 3. (a) Relationship between [18F] 2-fluoro-2-deoxy-D-glucose uptake and glucose transporter 1 expression in cholangiocellular carcinoma. A statistically significant difference in uptake was noted between glucose transporter 1-negative and -positive cells. PKM2, pyruvate kinase type M2. (b) Relationship between [18F] 2-fluoro-2-deoxy-D-glucose uptake and pyruvate kinase M2 expression in cholangiocellular carcinoma. No significant difference was observed between pyruvate kinase M2-negative and -positive cells. FDG, [18F] 2-fluoro-2-deoxy-D-glucose, SUV, standardized uptake value.

cancer cells. We examined whether PKM2 protein upregulation was linked to the clinical characteristics of ICC (Table 3). There was no correlation between PKM2 expression and maximum diameter, histological grading, T stage, or stage. However, PKM2 expression tended to correlate with lymph node metastasis (p = 0.051). Overall, 85.8% of patients with lymph node metastases had PKM2-positive tumours.

3.4. 18F-FDG uptake in relation to Glut-1 and PKM2 expression

In surgically resected masses, FDG uptake within the primary masses was compared with Glut-1 and PKM2 immunolabeling. We observed that Glut-1-positive tumours had higher SUVs than Glut-1-negative tumours (Fig. 3a). However, PKM2 expression was not correlated with SUV (Fig. 3b), and no significant correlation was observed between Glut-1 and PKM2 expression (p = 0.637, data not shown).

4. Discussion

The present study showed that FDG uptake is associated with tumour expression of Glut-1 but not PKM2. However, PKM2 tended to correlate with lymph node metastasis in patients with ICC. Collectively, these results suggest that PKM2 plays a pivotal role in balancing glucose metabolism and cellular growth.

ICC is associated with poor prognosis, and newly diagnosed patients are frequently found to have ICC that has progressed beyond surgery. The resectability of ICC remains low because of its early metastasis and advanced stage when diagnosed [29]. The postoperative 5-year survival rates have been reported to range from 20% to 30% [8]. Surgery for ICC often requires extended hepatic resection. We performed major hepatic resections in 73.4% (14/19) of the cases included in the present study. The patients who underwent major hepatectomy had a better prognosis than those who did not (p = 0.007), and lobectomy often increased the rate of radical resection (R0). We achieved radical resection in 31.6% of patients, with a median survival after R0 resection of 79 months compared to 18 months for R+ patients (p = 0.017). Alfredo et al. also reported that Curative resection of ICC is the only therapy that can achieve long-term survival [5]: they achieved curative resection (R0) in 83% of the patients and performed a major hepatic resection in 63%. On the other hand, it is difficult to make a prediction of the ICC patients with a better prognosis, because the unfavourable prognosis of ICC may be attributable to a lack of clear clinical signs and symptoms; therefore, it is important to identify predictive factors. Moreover,

Please cite this article in press as: Suzuki H, et al. Relationship between 18-F-fluoro-deoxy-D-glucose uptake and expression of glucose transporter 1 and pyruvate kinase M2 in intrahepatic cholangiocarcinoma. Dig Liver Dis (2015), http://dx.doi.org/10.1016/j.dld.2015.03.017

as cancer cell growth is heavily dependent on glucose as a major energy substrate, it is important to examine glucose metabolism in patients with ICC.

A better understanding of the association between FDG uptake and clinicopathological features will provide more information. We found a significant correlation between several tumour characteristics and FDG uptake. Specifically, tumour differentiation was strongly correlated with FDG uptake. Adler et al. reported that breast cancer patients with poorly differentiated tumours have significantly higher FDG uptake than patients with well or moderately differentiated tumours [30]. In line with this, we also observed fewer differentiated tumours with higher FDG uptakes, suggesting that FDG uptake allows indirect assessment of the differentiation degree in patients with ICC. Moreover, FDG uptake was strongly correlated with tumour size ($p = 0.011$). A significant relationship between tumour size and SUV has been reported in many studies and various organs [31]. The FDG-PET SUV determined on the basis of Ki67 expression plays an essential role in assessing the proliferative status of breast cancer [12]. A high growth rate requires increased glucose intake, and a large tumour could exhibit increased FDG uptake. Unlike other cancer types, we found no correlation between the SUV and regional lymph node metastasis or stage for ICC. This may be due to the limited number of patients in this series. However, we did observe a significant correlation between SUV and lymph node metastasis with regard to mass-forming type (data not shown).

We found a wide range of Glut-1 expression in ICC surgical specimens. We divided the tumours into two groups based on low (<10%) or high (>10%) numbers of Glut-1-positive cells in the tumour sample, and found a significant correlation between Glut-1 expression and histological grading. Moreover, Glut-1 expression was strongly correlated with the SUV of the primary tumour. In this study, positive Glut-1 expression was found in all patients with poorly differentiated carcinoma. Less differentiated tumours are surrounded by a hypoxic microenvironment, and hypoxia has the potential to inhibit tumour cell differentiation [32]. Moreover, low oxygen levels can influence the cellular phenotypes by altering the expression of specific genes and are generally thought to give cancer cells an advantage by promoting factors considered beneficial for tumour growth and survival [33]. Hypoxia inducible factor 1 (HIF-1) is overexpressed in low-oxygen environments and is the primary transcription factor mediating several physiological and biological changes, including Glut-1 overexpression. Aloj et al. also reported that hypoxia upregulates Glut-1 expression in vitro [34].

Hypoxia increases Glut-1 expression, which would result in increased FDG uptake. In this study, Glut-1 expression was strongly correlated with the maximum SUV ($p = 0.001$). Glut-1 expression is significantly and positively correlated with SUV in colorectal cancer [31]. 18F-FDG uptake in malignant tumours largely depends on the presence of facilitated glucose transporters including Glut-1 and hexokinase type II (HKII) [35]; glucose phosphorylation by HKII, which is downstream of Glut-1, is also important. On the other hand, Aloj and colleagues insisted that FDG uptake correlates better with the FDG-phosphorylating activity of mitochondrial preparations rather than the expression of Glut-1 or hexokinase I and II genes in vitro [34]. This suggests that there may be differences among cancers originating from different tissues with regard to glucose metabolism, such as glucose uptake, glucose transporter rates, and hexokinase activity in the glycolytic pathway.

Tumour cells convert large amounts of glucose to lactate, even in the presence of oxygen, as opposed to large amounts of ATP synthesis. This phenomenon of aerobic glycolysis has been termed the Warburg effect [20]. In the glycolytic process, pyruvate kinase (PK) catalyses the last reaction, which is the transfer of a high-energy phosphate group from phosphoenolpyruvate to ADP, yielding ATP and pyruvate. PKM2 is the predominant PK in proliferating cancer cells [36], and PKMS-expressing cells produce more lactate and consume less oxygen than cells expressing other PKs. Rapidly growing cells must take up glucose at a high rate and maintain a balance between energy production (e.g., ATP synthesis) and anabolic processes such as protein, lipid, and nucleic acid synthesis. PKM2 plays a critical role in aerobic glycolysis and allows proliferating cells to regulate their anabolic and catabolic metabolism needs [37]. In this study, we could not demonstrate a correlation between PKM2 and Glut-1 expression; however, PKM2 has a nonglycolytic function in addition to its role in glycolysis. PKM2 is found in both the cytoplasm and nucleus, where it is associated with chromatin [36]. Yang et al. reported that PKM2 nuclear translocation, facilitated by EGFR activation, promotes β-catenin transactivation, leading to increased expression of cyclinD1 and c-Myc [24]. In our study, we identified translocation from the cytoplasm to the nucleus in the ICC cell line. In addition to the regulation in the glycolytic process, PKM2 is subject to complex regulation both by oncogenes and a tumour suppressor [23].

We found a tendency towards a correlation between PKM2 expression and lymph node metastasis, which is regarded as an important prognostic factor for patients with ICC [8]. Park showed that vascular endothelial growth factor-C (VEGF-C) expression in cancer cells correlated with lymph node metastasis in ICC [38], and another group demonstrated increased matrix metalloproteinase-9 expression in ICC with lymphatic metastasis [39]. On the other hand, several studies have described the nonglycolytic functions of PKM2, e.g., it directly interacts with HIF-1 and promotes transactivation of HIF-1 target genes [40]. The PKM2 translocated into the nucleus in response to the epidermal growth factor (EGF) associates with β-catenin, and this complex leads to increased expression of cyclin D1 and c-Myc [24]. Nuclear PKM2 also acts as a protein kinase that can phosphorylate signal transducer and activator of transcription 3 (STAT3) and thereby activate the transcription of cancer-relevant genes [41]. Collectively, the evidence suggests that high PKM2 expression might be a key factor contributing to tumour cell invasion and metastasis, including lymph node metastases. Kimura et al. showed that HIF-1α expression is associated with vascular endothelial growth in human oesophageal squamous cell carcinoma [42] and plays a role in lymphatic invasion and lymph node metastasis through the induction of VEGF-C in oesophageal cancer. These findings are consistent with our results, which suggest that PKM2 might promote lymph node metastasis of ICC through cancer-relevant proteins such as HIF-1, STAT3, and β-catenin.

The cell-of-origin-based ICCs classification has shown the clinicopathological difference between Muc-ICCs and Mixed-ICCs [25]. Briefly, Muc-ICCs showed a more aggressive behaviour than Mixed-ICCs. Likewise, our study showed that the median survival time of 18.2 months in patients with muc-ICCs was shorter than the 98.7 months in patients with mixed-ICCs. In addition, patients with muc-ICCs tended to have poorer prognoses compared with patients with mixed-ICCs. However, there were no significant differences between the two groups. This may be also due to the small number of cases included. Nevertheless, 83% of patients with muc-ICCs showed positive Glut-1 expression. Glut-1 expression is increased under hypoxic conditions, and hypoxia is related to the inhibition of tumour cell differentiation. The patients with muc-ICC included 5 cases of poorly differentiated adenocarcinoma. Unfortunately, our data do not demonstrate a direct link between Glut-1 expression and muc-ICC. Further studies are needed to show a more convincing association.

In this study, Glut-1, but not PKM2 expression, strongly correlated with FDG uptake. PKM2 plays a variety of roles in addition to its glycolytic function, and may enhance tumour cell invasion and promote lymph node metastasis of ICC. However, further studies are required to clarify the energy metabolism and 18F-FDG uptake

Please cite this article in press as: Suzuki H, et al. Relationship between 18-F-fluoro-deoxy-D-glucose uptake and expression of glucose transporter 1 and pyruvate kinase M2 in intrahepatic cholangiocarcinoma. Dig Liver Dis (2015), http://dx.doi.org/10.1016/j.dld.2015.03.017

patterns in association with various oncogenic alterations that regulate glycolytic pathways, cancer proliferation, and tumourigenesis.

Conflict of interest

None declared.

References

[1] Lang H, Sotiropoulos GC, Fruhauf NR, et al. Extended hepatectomy for intrahepatic cholangiocellular carcinoma (ICC): when is it worthwhile? Single center experience with 27 resections in 50 patients over a 5-year period. Annals of Surgery 2005;241:134–43.
[2] Lang H, Sotiropoulos GC, Sgourakis G, et al. Operations for intrahepatic cholangiocarcinoma: single-institution experience of 158 patients. Journal of the American College of Surgeons 2009;208:218–28.
[3] Zhou XD, Tang ZY, Fan J, et al. Intrahepatic cholangiocarcinoma: report of 272 patients compared with 5,829 patients with hepatocellular carcinoma. Journal of Cancer Research and Clinical Oncology 2009;135:1073–80.
[4] Yedibela S, Demir R, Zhang W, et al. Surgical treatment of mass-forming intrahepatic cholangiocarcinoma: an 11-year Western single-center experience in 107 patients. Annals of Surgical Oncology 2009;16:404–12.
[5] Guglielmi A, Ruzzenente A, Campagnaro T, et al. Intrahepatic cholangiocarcinoma: prognostic factors after surgical resection. World Journal of Surgery 2009;33:1247–54.
[6] Hyder O, Hatzaras I, Sotiropoulos GC, et al. Recurrence after operative management of intrahepatic cholangiocarcinoma. Surgery 2013;153:811–8.
[7] Saxena A, Chua TC, Sarkar A, et al. Clinicopathologic and treatment-related factors influencing recurrence and survival after hepatic resection of intrahepatic cholangiocarcinoma: a 19-year experience from an established Australian hepatobiliary unit. Journal of Gastrointestinal Surgery 2010;14:1128–38.
[8] de Jong MC, Nathan H, Sotiropoulos GC, et al. Intrahepatic cholangiocarcinoma: an international multi-institutional analysis of prognostic factors and lymph node assessment. Journal of Clinical Oncology 2011;29:3140–5.
[9] Muros MA, Llamas-Elvira JM, Ramirez-Navarro A, et al. Utility of fluorine-18-fluorodeoxyglucose positron emission tomography in differentiated thyroid carcinoma with negative radioiodine scans and elevated serum thyroglobulin levels. American Journal of Surgery 2000;179:457–61.
[10] Tanaka T, Kawai Y, Kanai M, et al. Usefulness of FDG-positron emission tomography in diagnosing peritoneal recurrence of colorectal cancer. American Journal of Surgery 2002;184:433–6.
[11] Kluge R, Schmidt F, Caca K, et al. Positron emission tomography with [(18)F]fluoro-2-deoxy-D-glucose for diagnosis and staging of bile duct cancer. Hepatology 2001;33:1029–35.
[12] Gil-Rendo A, Martinez-Regueira F, Zornoza G, et al. Association between [18F]fluorodeoxyglucose uptake and prognostic parameters in breast cancer. British Journal of Surgery 2009;96:166–70.
[13] Seo S, Hatano E, Higashi T, et al. Fluorine-18 fluorodeoxyglucose positron emission tomography predicts lymph node metastasis: P-glycoprotein expression, and recurrence after resection in mass-forming intrahepatic cholangiocarcinoma. Surgery 2008;143:769–77.
[14] Lee JD, Yang WI, Park YN, et al. Different glucose uptake and glycolytic mechanisms between hepatocellular carcinoma and intrahepatic mass-forming cholangiocarcinoma with increased (18)F-FDG uptake. Journal of Nuclear Medicine 2005;46:1753–9.
[15] Yen TC, See LC, Lai CH, et al. 18F-FDG uptake in squamous cell carcinoma of the cervix is correlated with glucose transporter 1 expression. Journal of Nuclear Medicine 2004;45:22–9.
[16] Kunkel M, Reichert TE, Benz P, et al. Overexpression of Glut-1 and increased glucose metabolism in tumours are associated with a poor prognosis in patients with oral squamous cell carcinoma. Cancer 2003;97:1015–24.
[17] Amann T, Maegdefrau U, Hartmann A, et al. GLUT1 expression is increased in hepatocellular carcinoma and promotes tumourigenesis. American Journal of Pathology 2009;174:1544–52.
[18] Paudyal B, Oriuchi N, Paudyal P, et al. Expression of glucose transporters and hexokinase II in cholangiocellular carcinoma compared using [18F]-2-fluro-2-deoxy-D-glucose positron emission tomography. Cancer Science 2008;99:260–6.
[19] Haber RS, Rathan A, Weiser KR, et al. GLUT1 glucose transporter expression in colorectal carcinoma: a marker for poor prognosis. Cancer 1998;83:34–40.
[20] Warburg O, Wind F, Negelein E. The metabolism of tumours in the body. Journal of General Physiology 1927;8:519–30.
[21] Gatenby RA, Gillies RJ. Why do cancers have high aerobic glycolysis? Nature Reviews Cancer 2004;4:891–9.
[22] Christofk HR, Vander Heiden MG, Harris MH, et al. The M2 splice isoform of pyruvate kinase is important for cancer metabolism and tumour growth. Nature 2008;452:230–3.
[23] Tamada M, Suematsu M, Saya H. Pyruvate kinase M2: multiple faces for conferring benefits on cancer cells. Clinical Cancer Research 2012;18:5554–61.
[24] Yang W, Xia Y, Ji H, et al. Nuclear PKM2 regulates beta-catenin transactivation upon EGFR activation. Nature 2011;480:118–22.
[25] Komuta M, Govaere O, Vandecaveye V, et al. Histological diversity in cholangiocellular carcinoma reflects the different cholangiocyte phenotypes. Hepatology 2012;55:1876–88.
[26] Japan LCSGo classification of primary liver cancer. 1st English ed. Tokyo: Kanehara; 1997. p. 6–7.
[27] Sobin LH. TNM classification of malignant tumours. 6th ed. John Wiley & Sons; 2002.
[28] Kaira K, Endo M, Abe M, et al. Biologic correlation of 2-[18F]-fluoro-2-deoxy-D-glucose uptake on positron emission tomography in thymic epithelial tumours. Journal of Clinical Oncology 2010;28:3746–53.
[29] Endo I, Gonen M, Yopp AC, et al. Intrahepatic cholangiocarcinoma: rising frequency, improved survival, and determinants of outcome after resection. Annals of Surgery 2008;248:84–96.
[30] Adler LP, Crowe JP, al-Kaisi NK, et al. Evaluation of breast masses and axillary lymph nodes with [F-18] 2-deoxy-2-fluoro-D-glucose PET. Radiology 1993;187:743–50.
[31] Gu J, Yamamoto H, Fukunaga H, et al. Correlation of GLUT-1 overexpression: tumour size, and depth of invasion with 18F-2-fluoro-2-deoxy-D-glucose uptake by positron emission tomography in colorectal cancer. Digestive Diseases and Sciences 2006;51:2198–205.
[32] Kim Y, Lin Q, Glazer PM, et al. Hypoxic tumour microenvironment and cancer cell differentiation. Current Molecular Medicine 2009;9:425–34.
[33] Gomez-Casero E, Navarro M, Rodriguez-Puebla ML, et al. Regulation of the differentiation-related gene Drg-1 during mouse skin carcinogenesis. Molecular Carcinogenesis 2001;32:100–9.
[34] Aloj L, Caraco C, Jagoda E, et al. Glut-1 and hexokinase expression: relationship with 2-fluoro-2-deoxy-D-glucose uptake in A431 and T47D cells in culture. Cancer Research 1999;59:4709–14.
[35] Higashi T, Saga T, Nakamoto Y, et al. Relationship between retention index in dual-phase (18)F-FDG PET, and hexokinase-II and glucose transporter-1 expression in pancreatic cancer. Journal of Nuclear Medicine 2002;43:173–80.
[36] Mazurek S, Boschek CB, Hugo F, et al. Pyruvate kinase type M2 and its role in tumour growth and spreading. Seminars in Cancer Biology 2005;15:300–8.
[37] Mazurek S. Pyruvate kinase type M2: a key regulator of the metabolic budget system in tumour cells. International Journal of Biochemistry & Cell Biology 2011;43:969–80.
[38] Park BK, Paik YH, Park JY, et al. The clinicopathologic significance of the expression of vascular endothelial growth factor-C in intrahepatic cholangiocarcinoma. American Journal of Clinical Oncology 2006;29:138–42.
[39] Shirabe K, Shimada M, Kajiyama K, et al. Expression of matrix metalloproteinase-9 in surgically resected intrahepatic cholangiocarcinoma. Surgery 1999;126:842–6.
[40] Luo W, Hu H, Chang R, et al. Pyruvate kinase M2 is a PHD3-stimulated coactivator for hypoxia-inducible factor 1. Cell 2011;145:732–44.
[41] Gao X, Wang H, Yang JJ, et al. Pyruvate kinase M2 regulates gene transcription by acting as a protein kinase. Molecular Cell 2012;45:598–609.
[42] Kimura S, Kitadai Y, Tanaka S, et al. Expression of hypoxia-inducible factor (HIF)-1alpha is associated with vascular endothelial growth factor expression and tumour angiogenesis in human oesophageal squamous cell carcinoma. European Journal of Cancer 2004;40:1904–12.

Please cite this article in press as: Suzuki H, et al. Relationship between 18-F-fluoro-deoxy-D-glucose uptake and expression of glucose transporter 1 and pyruvate kinase M2 in intrahepatic cholangiocarcinoma. Dig Liver Dis (2015), http://dx.doi.org/10.1016/j.dld.2015.03.017

Cancer Chemother Pharmacol (2015) 75:569–577
DOI 10.1007/s00280-015-2676-0

ORIGINAL ARTICLE

A randomized phase II study of combination therapy with S-1, oral leucovorin, and oxaliplatin (SOL) and mFOLFOX6 in patients with previously untreated metastatic colorectal cancer

Kentaro Yamazaki · Hiroyuki Kuwano · Hitoshi Ojima · Toshio Otsuji · Takeshi Kato · Ken Shimada · Ichinosuke Hyodo · Tomohiro Nishina · Kuniaki Shirao · Taito Esaki · Takashi Ohishi · Tadamichi Denda · Masahiro Takeuchi · Narikazu Boku

Received: 27 November 2014 / Accepted: 3 January 2015 / Published online: 10 January 2015

Abstract
Purpose Biochemical modulation of 5-fluorouracil (5-FU) by leucovorin (LV) enhances antitumor activity. LV is thus often added to 5-FU-based regimens for the treatment of metastatic colorectal cancer (mCRC). A combination of S-1, oxaliplatin, and LV (SOL) was shown to be feasible, effective, and safe in a previous phase I trial. We therefore conducted a randomized phase II trial to evaluate efficacy and safety of SOL compared with mFOLFOX6.
Methods Patients with mCRC and no prior chemotherapy were randomly assigned to receive either SOL or mFOLFOX6. SOL consisted of S-1 (40–60 mg bid) plus oral LV (25 mg bid) for 1 week and oxaliplatin (85 mg/m^2) on day 1, repeated every 2 weeks.
Results Among 107 patients enrolled from July 2008 through July 2009, 105 (56 in the SOL group and 49 in the mFOLFOX6 group) were eligible and evaluated. The median progression-free survival was 9.6 months in the SOL group and 6.9 months in the mFOLFOX6 group [hazard ratio (HR) 0.83, 95 % confidence interval (CI) 0.49–1.40]. The median overall survival was 29.9 and 25.9 months, respectively (HR 0.91, 95 % CI 0.55–1.49). The response rate was 55 % in both groups. Grade 3 or 4 adverse drug reactions were neutropenia (20 % with SOL vs 41 % with mFOLFOX6), sensory neuropathy (20 vs 2.0 %), anorexia (13 vs 7.8 %), fatigue (11 vs 5.9 %), and diarrhea (11 vs 3.9 %).
Conclusions SOL demonstrated promising efficacy and acceptable toxicity as first-line chemotherapy for mCRC.

K. Yamazaki (✉)
Division of Gastrointestinal Oncology, Shizuoka Cancer Center, 1007 Shimonagakubo, Nagaizumi-cho, Sunto-gun, Shizuoka 411-8777, Japan
e-mail: k.yamazaki@scchr.jp

H. Kuwano
Department of General Surgical Science, Gunma University Hospital, Maebashi, Japan

H. Ojima
Gastro-intestinal Surgery, Gunma Prefectural Cancer Center, Ota, Japan

T. Otsuji
Department of Internal Medicine, Dongo Hospital, Yamatotakada, Japan

T. Kato
Department of Surgery, Minoh City Hospital, Minoh, Japan

Present Address:
T. Kato
Department of Surgery, Kansai Rosai Hospital, Amagasaki, Japan

K. Shimada
Department of Internal Medicine, Showa University Northern Yokohama Hospital, Yokohama, Japan

I. Hyodo
Division of Gastroenterology, University of Tsukuba, Tsukuba, Japan

T. Nishina
Department of Gastroenterology, National Hospital Organization Shikoku Cancer Center, Matsuyama, Japan

K. Shirao
Medical Oncology and Hematology, Faculty of Medicine, Oita University, Yufu, Japan

T. Esaki
Department of Gastrointestinal and Medical Oncology, National Kyusyu Cancer Center, Fukuoka, Japan

T. Ohishi
Department of Surgery, National Tokyo Medical Center, Tokyo, Japan

Further studies of SOL combined with molecular target agents are warranted.

Keywords Colorectal cancer · S-1 · LV · Leucovorin · Oxaliplatin

Introduction

Colorectal cancer (CRC) is the most common cancer in female and second in male in Japan, and there were 112,675 new cases of CRC and 49,345 deaths attributed to this disease in 2012 [1]. Fluorouracil (5-FU) is a key agent for the management of CRC. Its mode of action involves inhibition of thymidylate synthetase (TS) [2, 3]. Leucovorin (LV) is often combined as a biochemical modulator to enhance the efficacy of 5-FU [4]. This concept is based on the results of preclinical studies showing that 5-fluorodeoxyuridine monophosphate forms a ternary complex with TS, a key enzyme in DNA synthesis, in the presence of reduced folates, mainly 5,10-methylenetetrahydrofolate [5]. A meta-analysis including data on more than 3,000 patients revealed that LV improves response rates (RRs) and overall survival (OS) when combined with 5-FU, as compared with 5-FU alone [6].

Oxaliplatin (L-OHP) is a third-generation platinum compound associated with reduced toxicity and improved convenience compared to former generations of platinum compounds because hydration is not required. Randomized clinical trials have consistently shown that a regimen combining an intravenous infusion of 5-FU and *l*-LV with L-OHP (FOLFOX) produce higher RRs and a longer time to progression (TTP) than a combination of 5-FU and *l*-LV as first- or second-line treatment for advanced CRC. FOLFOX is one of global standard regimens for the first- and second-line chemotherapy of metastatic CRC (mCRC) [7–9].

S-1 is an oral fluoropyrimidine preparation combining tegafur (FT), 5-chloro-2, 4-dihydroxypyridine (CDHP), and potassium oxonate (Oxo). FT is a pro-drug of 5-FU, CDHP is a dihydropyrimidine dehydrogenase (DPD) inhibitor that acts to maintain higher levels of 5-FU in serum, and Oxo is an inhibitor of orotate phosphoribosyl transferase that reduces gastrointestinal toxicity caused by 5-FU. Phase II studies of single-agent S-1 conducted in late 1990s for patients with previously untreated mCRC reported RRs of 35–40 %, a median TTP of 5.3 months, and a median survival time (MST) of 12 months [10, 11]. In a phase II study of S-1 plus LV (2 weeks of treatment followed by 2 weeks of rest) in patients with CRC, the RR was 57 %, with a median TTP of 6.7 months and an MST of 24.3 months [12]. S-1 combined with LV has shown promising efficacy as compared with S-1 alone. The results of a phase I study evaluating a regimen combining S-1 and LV with L-OHP were reported in 2008 [13]. In that study, S-1 and LV were given daily for 1 week followed by a 1-week rest, and L-OHP was given every 2 weeks (SOL regimen). Five of all 6 patients who received the recommended doses of S-1 (40 mg, twice daily), LV (25 mg, twice daily), and L-OHP (85 mg/m^2) had confirmed partial responses (PRs), and dose-limiting toxic effects (grade 3 diarrhea and grade 3 hypertension) developed in 1 of the 6 patients. These results suggested that SOL may be an effective and tolerable regimen. We therefore performed a multicenter randomized phase II study to evaluate efficacy and safety of SOL compared with modified FOLFOX6 (mFOLFOX6) as a first-line treatment for mCRC.

Patients and methods

Patient selection

The eligibility criteria of this study were as follows: a histologically confirmed diagnosis of adenocarcinoma of the colon or rectum; unresectable metastatic disease; at least one measurable lesion according to the Response Evaluation Criteria in Solid Tumors (RECIST), version 1.0; adequate oral intake; an age of ≥20 years; no previous treatment for metastatic disease; an Eastern Cooperative Oncology Group performance status of 0 or 1; adequate bone marrow, liver, and renal functions; and written informed consent.

Patients were excluded if they had a history of serious hypersensitivity; active infection; serious concomitant diseases or conditions, such as severe ascites, pleural effusion, or pericardial effusion; extensive bone metastases; brain metastases or symptoms of brain metastases; diarrhea; sensory peripheral neuropathy; or another synchronous cancer.

Randomization

Patients were randomly assigned to receive SOL or mFOLFOX6 at a central registration center, using a minimization

T. Denda
Division of Gastroenterology, Chiba Cancer Center, Chiba, Japan

M. Takeuchi
Division of Biostatistics and Pharmaceutical Medicine, Department of Clinical Medicine, Kitasato University School of Pharmacy, Tokyo, Japan

N. Boku
Department of Clinical Oncology, St. Marianna University School of Medicine, Kawasaki, Japan

method with stratification according to disease status (unresectable or recurrent disease) and institution.

Procedures

This randomized, open-label, phase II study in patients with mCRC was conducted in 22 institutions in Japan. Patients in the mFOLFOX6 group received a concurrent intravenous infusion of L-OHP (85 mg/m^2) and *l*-LV (200 mg/m^2) and then a bolus injection of 5-FU (400 mg/m^2) on day 1, followed by a continuous intravenous infusion of 5-FU (2,400 mg/m^2) over 46 h, repeated every 2 weeks. Patients in the SOL group received an intravenous infusion of L-OHP (85 mg/m^2) on day 1 every 2 weeks, and S-1 and LV were given together orally twice daily for 1 week, followed by 1-week rest. The dose of S-1 was assigned according to body surface area as follows: <1.25 m^2, 40 mg; 1.25 to <1.50 m^2, 50 mg; and ≥1.50 m^2, 60 mg, twice daily. The dose of LV was fixed at 25 mg twice daily.

Dose reduction and/or cycle delays were permitted according to predefined toxicity criteria. In both the mFOLFOX6 and SOL groups, treatment was delayed until the resolution of adverse events in the previous cycle to the following values: neutrophil count ≥1,500/mm^3, platelets ≥75,000/mm^3, creatinine ≤1.5 mg/dL, diarrhea, stomatitis, or rash ≤grade 1, and sensory peripheral neuropathy ≤grade 2. If grade 4 leukopenia, thrombocytopenia, or grade 3 or higher febrile neutropenia, diarrhea, or sensory peripheral neuropathy occurred, the dose of the drug(s) to which the adverse event was attributed was reduced by one level for the next cycle of chemotherapy. The protocol treatment was continued until disease progression, unacceptable toxicity, or the patient's refusal.

Physical examinations and laboratory tests were performed at baseline and were repeated every week during the first four cycles of chemotherapy and every 2 weeks from the fifth cycle onward. Tumors were assessed every 6 weeks until disease progression. Tumor response was evaluated according to the RECIST criteria version 1.0. For PR or complete response (CR), response was confirmed by assessments with no less than 4 weeks of interval after the criteria for response were first met. Progression-free survival (PFS) was defined as the time from randomization to disease progression or death from any cause. Data on patients without documented evidence of progressive disease or death were censored on the date of the last tumor assessment without progression during the protocol treatment. Response and PFS were evaluated by an independent review committee (IRC). OS was calculated from the date of randomization to the date of death from any cause. Toxicity was evaluated according to the Common Terminology Criteria for Adverse Events (CTCAE), version 3.0.

Pharmacokinetic analysis

On day 1 of the first cycle of treatment, blood samples for pharmacokinetic analysis of S-1, LV, and L-OHP were collected before and after administration of these drugs. Plasma concentrations of FT, 5-FU, CDHP, Oxo, LV, and 5-methyltetrahydrofolate (5-MeTHF) were quantified as reported previously [14, 15], and platinum concentrations in plasma ultrafiltrate, total plasma, and red blood cells (RBC) were determined by inductively coupled plasma mass spectrometry (ICP-MS). Pharmacokinetic variables, maximum concentration (C_{max}), time to reach C_{max} (T_{max}), area under the concentration–time curve (AUC_{∞}), and elimination half-life ($T_{1/2}$) were calculated by noncompartmental model analysis, performed with the use of WinNonlin, version 5.2 (Pharsight Corporation, Cary, NC, USA).

Statistical analysis

The primary end point was to estimate the treatment effect on PFS of SOL relative to mFOLFOX6. The median PFS was assumed to be 10.0 months in SOL group and 8.0 months in the mFOLFOX6 group (hazard ratio [HR], 0.8) based on the results of previous reports [7, 16, 17]. The sample size was set to achieve a probability of 80 % or higher that a point estimate of the HR for PFS is less than 1.0. The number of events of PFS required for primary analysis was set at 74. Thus, the sample size calculated with a Monte Carlo simulation was 106 patients. Secondary end points were OS, RR, disease control rate [DCR; CR + PR + stable disease (SD)], pharmacokinetics, and toxicity. PFS and OS curves were estimated using the Kaplan–Meier method. A stratified log-rank test adjusted by disease stage (unresectable or postoperative recurrence) was used for comparisons between two groups, and a Cox proportional hazard model was used to estimate HRs and two-tailed 95 % confidence intervals (CIs). The 95 % CIs for median PFS and OS were calculated with the method of Brookmeyer and Crowley. All *P* values are two-sided. All statistical analyses were done with SAS version 8.2 software (SAS Institute, Inc., Cary, NC, USA).

The study was approved by the institutional review board at each participating center. Throughout the study, an independent data-monitoring committee monitored the safety. The study was performed in accordance with the Declaration of Helsinki and Japanese Good Clinical Practice Guidelines and registered at ClinicalTrials.gov and given the identifier number of NCT00721916.

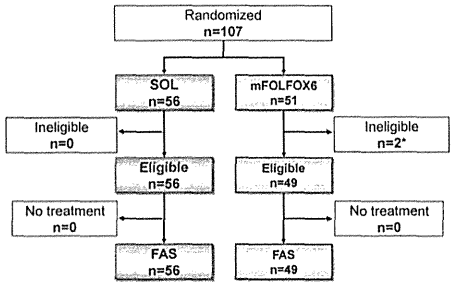

Fig. 1 CONSORT diagram. *Asterisk* no target lesion by independent review committee. mFOLFOX6, modified FOLFOX6; FAS, full analysis set; SOL, S-1, leucovorin, and oxaliplatin

Results

Patient characteristics

From July 2008 through July 2009, a total of 107 patients were randomly assigned to each treatment group. Fifty-six patients were assigned to the SOL group and 51 patients to the mFOLFOX6 group (Fig. 1). Two patients in mFOLFOX6 group who were judged to have no measurable lesions by the IRC were excluded from analysis. The characteristics of the 105 eligible patients are shown in Table 1. Patient characteristics were well balanced between the two arms, except for gender.

Treatment exposure and subsequent treatment

The median number of administered treatment cycles was 12 (range 1–63) in the SOL group and 11 (range 1–69) in the mFOLFOX6 group. The reasons for treatment discontinuation were disease progression in 41 patients (73.2 %) in the SOL group and 41 (83.7 %) in the mFOLFOX6 group, adverse events in 14 patients (25.0 %) in the SOL group and 2 (4.1 %) in the mFOLFOX6 group, and surgery in 1 patient (1.8 %) in the SOL group and 5 (10.2 %) in the mFOLFOX6 group.

Efficacy

The cutoff date for PFS was March 31, 2010. OS was followed until January 31, 2012, resulting in a median follow-up time of 35 months. Median PFS (assessed by the IRC) was 9.6 months in the SOL group and 6.9 months in the mFOLFOX6 group. For PFS (assessed by the IRC), the HR for SOL versus mFOLFOX6 was 0.83 (95 % CI 0.49–1.40), which met the criterion for evidence of activity (HR < 1.0) as predefined in the protocol (Fig. 2a).

Table 1 Patient characteristics

	SOL ($n = 56$)		mFOLFOX6 ($n = 49$)	
	n	%	*n*	%
Gender				
Male	33	58.9	23	46.9
Female	23	41.1	26	53.1
Age (years)				
Median	60.5		61.0	
Range	27–77		27–76	
PS				
0	49	87.5	40	81.6
1	7	12.5	9	18.4
Diagnosis				
Colon	36	64.3	27	55.1
Rectum	20	35.7	21	42.9
Colon/rectum	0	0.0	1	2.0
Stage				
Unresectable	42	75.0	38	77.6
Recurrent	14	25.0	11	22.4
Number of metastatic sites				
1	24	42.9	20	40.8
2	19	33.9	21	42.9
3≤	13	23.2	8	16.3

mFOLFOX6 modified FOLFOX6, *PS* performance status, *SOL* S-1, leucovorin, and oxaliplatin

The proportion of patients who received subsequent therapy was slightly higher in the SOL group (100 %) than in the mFOLFOX6 group (91.8 %). Irinotecan was given to 37 patients (66.1 %) in the SOL group and 33 (67.3 %) in the mFOLFOX6 group, bevacizumab to 26 patients (46.4 %) in the SOL group and 19 (38.8 %) in the mFOLFOX6 group, and L-OHP to 12 (21.4 %) in the SOL group and 3 (6.1 %) in the mFOLFOX6 group.

Median OS was 29.9 months in the SOL group and 25.9 months in the mFOLFOX6 group (HR 0.91, 95 % CI 0.55–1.49; Fig. 2b).

Response is summarized in Table 2. The RRs were similar in the two treatment groups (55.4 % for SOL vs 55.1 % for mFOLFOX6). The DCR was slightly higher in the SOL group than in the mFOLFOX6 group (92.9 vs 85.7 %; $P = 0.340$). Individual responses to treatment are shown in Fig. 3. The patients who achieved a CR or PR at 6 weeks were seen in 41.1 % in the SOL group versus 20.4 % in the mFOLFOX6 group. The median time to response was shorter in the SOL group than in the mFOLFOX6 group (43.0 vs 78.0 days; $P = 0.055$). The median duration of response was 233.5 days in the SOL group and 132.0 days in the mFOLFOX6 group ($P = 0.795$).

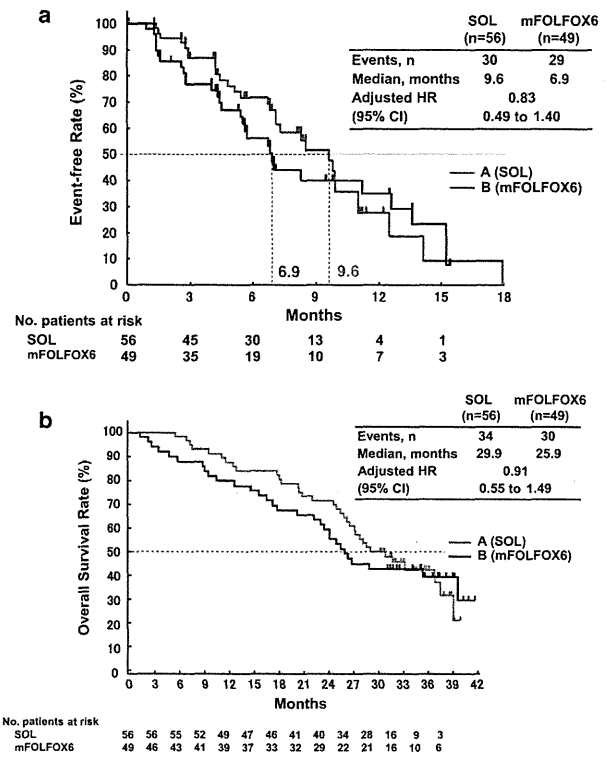

Fig. 2 Kaplan–Meier plots of **a** progression-free survival as evaluated by the independent review committee (IRC) on treatment (primary analysis; cutoff date, March 31, 2010) and **b** overall survival (final analysis). HR, hazard ratio; mFOLFOX6, modified FOLFOX6; SOL, S-1, leucovorin, and oxaliplatin

Safety

There were no treatment-related deaths in either treatment group. The incidences of adverse drug reactions in each group are summarized in Table 3. Common grade 3 or 4 adverse drug reactions with an incidence that was 5 or more percentage points higher in the SOL group than in the mFOLFOX6 group were anemia, diarrhea, colitis, stomatitis, nausea, and peripheral sensory neuropathy. On the other hand, grade 3 or 4 neutropenia was more common in the mFOLFOX6 group than in the SOL group. About 20 % of the patients ($n = 11$) had grade 3 sensory neurotoxicity in the SOL group. In 6 of these patients (54.5 %), grade 3 neuropathy improved within 2 weeks. Overall, 62.5 % of the patients had grade 3 or 4 toxicity in the SOL group, as compared with 56.9 % in the mFOLFOX6 group. Serious adverse events occurred in 21.4 % of the patients in the SOL group and 23.5 % of those in the mFOLFOX6 group.

Dose intensity

In the SOL group, the median relative dose intensity was 72.6 % for S-1 and 71.0 % for L-OHP. In the mFOLFOX6 group, the median relative dose intensity was 75.7 % for bolus 5-FU, 79.2 % for infusional 5-FU, and 68.8 % for L-OHP. The median cumulative doses of L-OHP for 6 cycles, 12 cycles, and during the entire treatment period were, respectively, 510.0, 777.5, and 807.5 mg/m^2 in the SOL group and 450.0, 715.0, and 755.0 mg/m^2 in the mFOLFOX6 group. The proportion of patients in whom the cumulative dose of L-OHP exceeded 800 mg/m^2 was higher in the SOL group (50.0 %) than in the mFOLFOX6 group (40.8 %).

Pharmacokinetics

Six patients in the SOL group underwent pharmacokinetic analysis of S-1, LV, and platinum (Appendix Tables 4

Table 2 Response rates

	SOL ($n = 56$)		mFOLFOX6 ($n = 49$)		*P* value
	n	(%)	*n*	(%)	
CR	1	1.8	0	0.0	
PR	30	53.6	27	55.1	
SD	21	37.5	15	30.6	
PD	4	7.1	7	14.3	
RR	31	55.4	27	55.1	1.000*
95 % CI (%)		41.5–68.7		40.2–69.3	
DCR	52	92.9	42	85.7	0.340*
95 % CI (%)		82.7–98.0		72.8–94.1	
Median time to first response, days	43.0		78.0		0.055**

According to RECIST 1.0. Assessed by independent review committee

CI confidence interval, *CR* complete response, *DCR* disease control rate, *mFOLFOX6* modified FOLFOX6 (fluorouracil, leucovorin, and oxaliplatin), *PD* progressive disease, *PR* partial response, *PS* performance status, *RR* response rate, *SD* stable disease, *SOL* S-1, leucovorin, and oxaliplatin

* Fisher's exact test; ** *t* test

and 5). Six patients in the mFOLFOX6 group underwent pharmacokinetic analysis of platinum (Appendix Table 4). Plasma concentrations of all compounds peaked between 1.3 and 2.0 h after administration, and 5-FU, CDHP, Oxo, and 5-MeTHF were rapidly eliminated with the mean of $T_{1/2}$ values of 1.8, 2.5, 2.2, and 2.3 h, respectively. The pharmacokinetic profiles of platinum in plasma ultrafiltrate, total plasma, and RBC in the SOL group were similar to those in the mFOLFOX6 group.

Discussion

Replacement of infusional 5-FU by an oral fluoropyrimidine provides a convenient treatment option for patients with mCRC, and capecitabine has been included in standard regimens globally. S-1 has also been developed mainly in Japan for the management of mCRC. A combination of S-1 and L-OHP (SOX) has shown promising antitumor activity in a phase II trial in patients with mCRC [18]. In a Korean phase III trial comparing SOX with capecitabine plus L-OHP (XELOX), the RR was significantly higher in the SOX group (47 %) than in the XELOX group (36 %; odds ratio, 1.68; 95 % CI, 1.05–2.69; $P = 0.0120$) and the noninferiority of SOX group to XELOX group in terms of PFS was shown [19]. Furthermore, SOX plus bevacizumab was shown to be noninferior to mFOLFOX6 plus bevacizumab in a phase III trial (SOFT trial) [20]. On the basis of the results of these pivotal phase III trials, SOX is considered to be an alternative treatment regimen for the

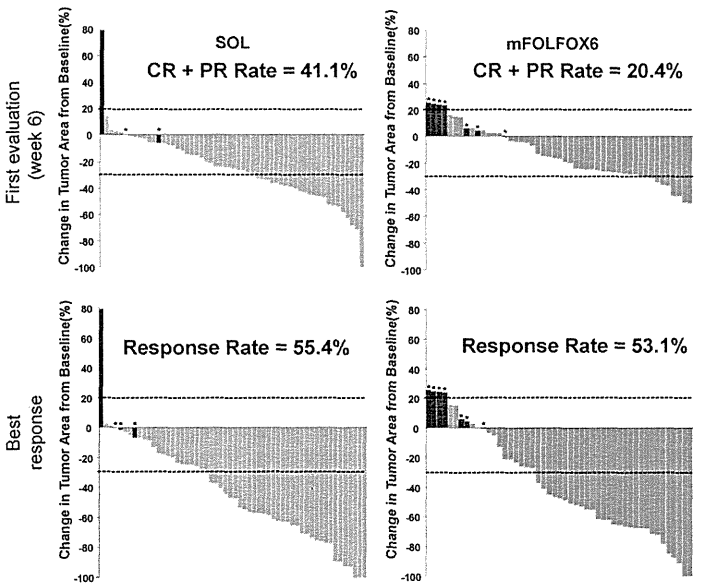

Fig. 3 Waterfall plots of the changes in target lesions from baseline at the first evaluation (week 6) or the best response in the S-1, leucovorin, and oxaliplatin (SOL) group and the modified FOLFOX6 (mFOLFOX6) group. (*Asterisk*) *Black lines* were assessed as progressive disease. PR, partial response

Table 3 Adverse drug reactions (safety analysis population)

Adverse event	SOL ($n = 56$), %				mFOLFOX6 ($n = 51$), %			
	Any	G3	G4	G3–4	Any	G3	G4	G3–4
Neutropenia	69.6	17.9	1.8	19.6	86.3	31.4	9.8	41.2
Leukopenia	53.6	5.4	0.0	5.4	72.5	3.9	0.0	3.9
Lymphopenia	51.8	12.5	1.8	14.3	41.2	3.9	2.0	5.9
Anemia	46.4	5.4	1.8	7.1	33.3	2.0	0.0	2.0
Thrombocytopenia	67.9	0.0	0.0	0.0	70.6	3.9	0.0	3.9
Febrile neutropenia	0.0	0.0	0.0	0.0	3.9	3.9	0.0	3.9
Diarrhea	69.6	10.7	0.0	10.7	45.1	3.9	0.0	3.9
Colitis	8.9	5.4	0.0	5.4	0.0	0.0	0.0	0.0
Stomatitis	71.4	7.1	0.0	7.1	54.9	0.0	0.0	0.0
Nausea	67.9	5.4	0.0	5.4	64.7	0.0	0.0	0.0
Fatigue	87.5	10.7	0.0	10.7	74.5	5.9	0.0	5.9
Anorexia	87.5	12.5	0.0	12.5	72.5	7.8	0.0	7.8
Peripheral sensory neuropathy	98.2	19.6	0.0	19.6	88.2	2.0	0.0	2.0

G grade, *mFOLFOX6* modified FOLFOX6, *SOL* S-1, leucovorin, and oxaliplatin

treatment of mCRC. The addition of LV to SOX (SOL) is expected to enhance the antitumor activity of SOX.

Our study evaluated efficacy and safety of SOL compared with mFOLFOX6 for the first-line treatment of mCRC. Median PFS was favorable in the SOL group compared with the mFOLFOX6 group. Although there were no differences in RRs, the response duration was substantially longer in SOL group than that in mFOLFOX6 group. The number of events related to PFS within 9 months and OS within 2 years after starting chemotherapy were substantially lower in the SOL group than in the mFOLFOX6 group.

Furthermore, the time to response in the SOL group came earlier than that in the mFOLFOX6 group. The patients who achieved a CR or PR at 6 weeks were seen in 41.1 % in the SOL group and 20.4 % in mFOLFOX6 group, and fewer patients had early disease progression (within 6 weeks) in the SOL group than in the mFOLFOX6 group. The correlation between earlier tumor shrinkage and survival (OS or PFS) in first-line chemotherapy of mCRC has been suggested as previously reported [21]. It is speculated that early tumor shrinkage and lower risk of earlier disease progression might contribute to preferable outcomes of SOL group in this study.

Molecular target agents have recently been shown to be effective in patients with mCRC, and regimens combining bevacizumab with FOLFOX, XELOX, or SOX appear particularly promising [20, 22]. Furthermore, the PFS and OS in the SOL group were similar to those reported for SOX plus bevacizumab and mFOLFOX6 plus bevacizumab [20]. SOL is expected to become a promising platform for combination with molecular target agents. Subsequently to this study, we conducted a phase II trial of combination therapy with SOL and bevacizumab in patients with mCRC [23]. In this phase II study, RR was 86 %, median PFS was 15 months, and 2-year survival rate was 72 %. There was no treatment death. Although the study was a small, single-arm phase II trial, the results suggested that SOL plus bevacizumab is safe and effective.

The incidence of treatment discontinuation due to adverse events was higher in the SOL group than that in the mFOLFOX6 group. Six of 14 patients in the SOL group discontinued protocol treatment due to hematological toxicities, such as neutropenia and thrombocytopenia, although grade 3 or 4 these adverse events were less frequent in the SOL group than in the mFOLFOX6 group. In previous phase I/II study of SOX, treatment discontinuation due to delayed recovery from hematological toxicities was observed in 8 of 32 patients (25 %) [18]. Therefore, it might be important to pay attention to this delayed recovery from hematological toxicities in SOL regimen. On the other hand, treatment discontinuation due to non-hematological toxicity was observed in only 1 patient of the SOL group (grade 3 anorexia and stomatitis), although grade 3 or 4 diarrhea, stomatitis, colitis, nausea, and peripheral sensory neuropathy were more common in the SOL group than in the mFOLFOX6 group. These toxicities were manageable by dose reduction in the subsequent treatment cycle. These adverse events causing treatment discontinuation recovered soon, and the 3 patients received subsequent chemotherapy after discontinuation of study treatment. It was well known that the incidence of gastrointestinal toxicities of 5-FU was high in Caucasian compared to Asian. The recommended dose of S-1 monotherapy in Caucasian was lower than Asian. When considering the development of SOL regimen in western countries, reassessment of dose and/or schedule of SOL would be necessary.

The incidence of grade 3 peripheral sensory neuropathy was higher in the SOL group than in the mFOLFOX6 group (19.6 vs 2.0 %). The results of pharmacokinetic analysis in our study indicated that there were no pharmacokinetic interactions among S-1, LV, and L-OHP. Drug interactions were unlikely to cause the high incidence of neuropathy in the SOL group. In SOFT trial which compared S-1 plus L-OHP plus bevacizumab with mFOLFOX6 plus bevacizumab, the grade 3 peripheral sensory neuropathy was observed in 14 % of patients, and the dose reduction of L-OHP was required in 57 % of patients, resulting in the relative dose intensity of L-OHP of 62.7 % in mFOLFOX6 plus bevacizumab. In our study, the relative dose intensity of L-OHP in SOL group was 71.0 %, and the cumulative dose of L-OHP in the SOL group was slightly higher than that in the mFOLFOX6 group. The incidence of grade 3 peripheral neuropathy in the SOL group was compatible with that of previously reported FOLFOX studies. It was unclear why the incidence of grade 3 peripheral sensory neuropathy was very low in the mFOLFOX6 group in this study. If appropriate dose modification or interruption of L-OHP (stop and go strategy) was applied to the SOL treatment in this study, it could be easier to manage neuropathy.

In conclusion, SOL showed favorable survival with earlier tumor shrinkage, as compared with mFOLFOX6 in our randomized phase II study. The toxicities were generally tolerable, although the incidence of nonhematological toxicities was higher than that with mFOLFOX6. Further studies of SOL combined with molecular target agents are warranted.

Acknowledgments We thank all the patients, their families, the investigators, and the medical staff. We are grateful to Yoshihiko Machara, Keisuke Aiba, Atsushi Sato for their kind advice as members of the Independent Data and Safety Monitoring Committee and Junji Tanaka, Kohki Yoshikawa, Takayuki Yoshino as members of the Independent Review Committee. We also thank Yuh Sakata for his advice as the medical advisor. Statistical data analysis was performed by Takanori Tanase, Taiho Pharmaceutical Co., Ltd.

Ethical standard I.H. has reported having an advisory role at Taiho Pharmaceutical Co., Ltd. and Yakult Honsha Co., Ltd. KShimada, TOishi, and M.T. have reported having an advisory role at Taiho Pharmaceutical Co., Ltd. KY, H.K., H.O., KShimada, I.H., T.N., KShirao, T.E., T.D., and N.B. have reported receiving honoraria from Taiho Pharmaceutical Co., Ltd. and Yakult Honsha Co., Ltd. TOhishi has reported receiving honoraria from Taiho Pharmaceutical Co., Ltd. K.Y., H.K., K. Shimada, I.H., T.N., K. Shirao, T.E., and T.D. have reported receiving research funding from Taiho Pharmaceutical Co., Ltd. and Yakult Honsha Co., Ltd. H.O., T. Otsuji, T.K., T. Ohishi, and N.B. have reported receiving research funding from Taiho Pharmaceutical Co., Ltd. All procedures performed in this study were in accordance with the ethical standards of the institutional review board at each participating center and with the 1964 Declaration of Helsinki and Japanese Good Clinical Practice Guidelines.

Informed consent Written informed consent was obtained from all individual participants included in this study.

Appendix

See Tables 4 and 5.

Table 4 Platinum pharmacokinetics in the SOL group and the mFOLFOX6 group

	n	Platinum concentrations in total plasma			Platinum concentrations in total plasma		
		C_{max} (ng/mL)	95% CI (ng/mL)	*P* value	$AUC_{0\text{-last}}$ (ng h/mL)	95% CI (ng h/mL)	*P* value
SOL	6	2,312 ± 409	2,018–2,586	0.7819	176,269 ± 26,040	155,484–196,359	0.8229
mFOLFOX6	6	2,347 ± 254	2,064–2,644		172,685 ± 19,967	152,863–193,049	
	n	Platinum concentrations in plasma ultrafiltrate			Platinum concentrations in plasma ultrafiltrate		
		C_{max} (ng/mL)	95% CI (ng/mL)	*P* value	$AUC_{0\text{-last}}$ (ng h/mL)	95% CI (ng h/mL)	*P* value
SOL	6	1,163 ± 181	967–1,372	0.2383	16,899 ± 3,633	13,632–20,119	0.7721
mFOLFOX6	6	1,023 ± 225	841–1,193		16,236 ± 3,200	13,140–19,392	
	n	Platinum concentrations in red blood cells			Platinum concentrations in red blood cells		
		C_{max} (ng/mL)	95% CI (ng/mL)	*P* value	$AUC_{0\text{-last}}$ (ng h/mL)	95% CI (ng h/mL)	*P* value
SOL	6	1,017 ± 79	909–1,131	0.3	193,157 ± 29,917	166,975–218,994	0.1117
mFOLFOX6	6	1,104 ± 158	981–1,220		224,083 ± 32,094	194,017–254,460	

AUC0-last: AUC0-336

The *P* values were determined by one-way ANOVA

CI confidence interval, *mFOLFOX6* modified FOLFOX6 (fluorouracil, leucovorin, and oxaliplatin), *SOL* S-1, leucovorin, and oxaliplatin

Table 5 LV and 5-MeTHF pharmacokinetics in the SOL group

	n	LV		LV	
		C_{max} (ng/mL)	95% CI (ng/mL)	$AUC_{0\text{-last}}$ (ng h/mL)	95% CI (ng h/mL)
SOL	6	507.7 ± 227.7	329.8–669.7	2,768.2 ± 1,355.5	1,771.5–3,624.2
	n	5-MeTHF		5-MeTHF	
		C_{max} (ng/mL)	95% CI (ng/mL)	$AUC_{0\text{-last}}$ (ng h/mL)	95% CI (ng h/mL)
SOL	6	461.4 ± 122.6	326.3–618.6	1951.0 ± 560.0	1,359.8–2,621.2

AUC0-last: AUC0-8

CI confidence interval, *LV* leucovorin, *5-MeTHF* 5-methyltetrahydrofolate, *SOL* S-1, leucovorin, and oxaliplatin

References

1. International Agency for Research on Cancer, World Health Organization. GLOBOCAN 2012. [Cited 31 Jul 2014]. http://globocan.iarc.fr/
2. Pinedo HM, Peters GF (1988) Fluorouracil: biochemistry and pharmacology. J Clin Oncol 6:1653–1664
3. Matsuoka H, Ueo H, Sugimachi K, Akiyoshi T (1992) Preliminary evidence that incorporation of 5-fluorouracil into RNA correlates with antitumor response. Cancer Invest 10:265–269
4. Advanced Colorectal Cancer Meta-Analysis Project (1992) Modulation of fluorouracil by leucovorin in patients with advanced colorectal cancer: evidence in terms of response rate. Advanced Colorectal Cancer Meta-Analysis Project. J Clin Oncol 10:896–903
5. Rustum YM, Trave F, Zakrzewski SF et al (1987) Biochemical and pharmacologic basis for potentiation of 5-fluorouracil action by leucovorin. NCI Monogr 4:165–170
6. Thirion P, Michiels S, Pignon JP et al (2004) Modulation of fluorouracil by leucovorin in patients with advanced colorectal cancer: an updated meta-analysis. J Clin Oncol 22:3766–3775
7. De Gramont A, Figer A, Seymour M et al (2000) Leucovorin and fluorouracil with or without oxaliplatin as first-line treatment in advanced colorectal cancer. J Clin Oncol 18:2938–2947
8. Rothenberg ML, Oza AM, Bigelow RH et al (2003) Superiority of oxaliplatin and fluorouracil-leucovorin compared with either therapy alone in patients with progressive colorectal cancer after irinotecan and fluorouracil-leucovorin: interim results of a phase III trial. J Clin Oncol 21:2059–2069
9. Goldberg RM, Sargent DJ, Morton RF et al (2004) A randomized controlled trial of fluorouracil plus leucovorin, irinotecan, and oxaliplatin combinations in patients with previously untreated metastatic colorectal cancer. J Clin Oncol 22:23–30
10. Ohtsu A, Baba H, Sakata Y et al (2000) Phase II study of S-1, a novel oral fluorophyrimidine derivative, in patients with metastatic colorectal carcinoma. S-1 Cooperative Colorectal Carcinoma Study Group. Br J Cancer 83:141–145
11. Shirao K, Ohtsu A, Takada H et al (2004) Phase II study of oral S-1 for treatment of metastatic colorectal carcinoma. Cancer 100:2355–2361
12. Koizumi W, Boku N, Yamaguchi K et al (2010) Phase II study of S-1 plus leucovorin in patients with metastatic colorectal cancer. Ann Oncol 21:766–771
13. Yamazaki K, Yoshino T, Boku N et al (2008) Phase I/II study of S-1/LV plus oxaliplatin (SOL) for untreated metastatic colorectal cancer: preliminary report of the phase I part. Proc Am Soc Clin Oncol 26:15101
14. Matsushima E, Yoshida K, Kitamura R, Yoshida K-I (1997) Determination of S-1 (combined drug of tegafur, 5-chloro-2,4-dihydroxypyridine and potassium oxonate and 5-fluorouracil in human plasma and urine using high-performance liquid chromatography and gas chromatography-negative ion chemical ionization mass spectrometry. J Chromatogr B Biomed Sci Appl 691:95–104
15. Shirao K, Hoff PM, Ohtsu A et al (2004) Comparison of the efficacy, toxicity, and pharmacokinetics of a uracil/tegafur (UFT) plus oral leucovorin (LV) regimen between Japanese and American patients with advanced colorectal cancer: joint United States and Japan study of UFT/LV. J Clin Oncol 22:3466–3474
16. Giacchetti S, Perpoint B, Zidani R et al (2000) Phase III multicenter randomized trial of oxaliplatin added to chronomodulated fluorouracil-leucovorin as first-line treatment of metastatic colorectal cancer. J Clin Oncol 18:136–147
17. Tournigand C, André T, Achille E et al (2004) FOLFIRI followed by FOLFOX6 or the reverse sequence in advanced colorectal cancer: a randomized GERCOR study. J Clin Oncol 22:229–237
18. Yamada Y, Tahara M, Miya T et al (2008) Phase I/II study of oxaliplatin with oral S-1 as first-line therapy for patients with metastatic colorectal cancer. Br J Cancer 98:1034–1038
19. Hong YS, Park YS, Lim HY et al (2012) S-1 plus oxaliplatin versus capecitabine plus oxaliplatin for first-line treatment of patients with metastatic colorectal cancer: a randomised, non-inferiority phase 3 trial. Lancet Oncol 13:1125–1132
20. Yamada Y, Takahari D, Matsumoto H et al (2013) Leucovorin, fluorouracil, and oxaliplatin plus bevacizumab versus S-1 and oxaliplatin plus bevacizumab in patients with metastatic colorectal cancer (SOFT): an open-label, non-inferiority, randomised phase 3 trial. Lancet Oncol 14:1278–1286
21. Giessen C, Laubender RP, Fischer von Weikersthal L et al (2013) Early tumor shrinkage in metastatic colorectal cancer: retrospective analysis from an irinotecan-based randomized first-line. Cancer Sci 6:718–724
22. Saltz LB, Clarke S, Díaz-Rubio E et al (2008) Bevacizumab in combination with oxaliplatin-based chemotherapy as first-line therapy in metastatic colorectal cancer: a randomized phase III study. J Clin Oncol 26:2013–2019
23. Yamazaki K, Nishina T, Kato T et al (2014) Final results of phase II study of S-1, oral leucovorin, oxaliplatin, and bevacizumab combination therapy (SOL + BV; SOLA) in metastatic colorectal cancer (mCRC). J Clin Oncol 32 (3 suppl; abstr 574)

OXFORD

Carcinogenesis, 2015, Vol. 36, No. 3, 338–345

doi:10.1093/carcin/bgu242
Advance Access publication December 10, 2014
Original Manuscript

ORIGINAL MANUSCRIPT

MicroRNA-7 expression in colorectal cancer is associated with poor prognosis and regulates cetuximab sensitivity via *EGFR* regulation

Toshinaga Suto, Takehiko Yokobori*, Reina Yajima, Hiroki Morita, Takaaki Fujii, Satoru Yamaguchi, Bolag Altan, Souichi Tsutsumi, Takayuki Asao and Hiroyuki Kuwano

Department of General Surgical Science, Graduate School of Medicine, Gunma University, 3-39-22 Showamachi, Maebashi 371-8511, Japan

*To whom correspondence should be addressed. Tel: +81-027-220-8224; Fax: +81-027-220-8230; Email: bori45@gunma-u.ac.jp

Abstract

MicroRNA-7 (*miR-7*) has been reported to be a tumor suppressor in all malignancies including colorectal cancer (CRC). However, its significance for CRC clinical outcomes has not yet been explored. The potential for *miR-7* to act as a tumor suppressor by coordinately regulating the epidermal growth factor receptor (*EGFR*) signaling pathway at several levels was examined. We investigated the tumor inhibitory effect of *miR-7* in CRC, with particular focus on the relationship between *miR-7* and the *EGFR* pathway. Quantitative reverse transcription–PCR was used to evaluate *miR-7* expression in 105 CRC cases to determine the clinicopathologic significance of this miRNA. The regulation of *EGFR* by *miR-7* was examined with *miR-7* precursor-transfected cells. Furthermore, we investigated whether *miR-7* suppresses proliferation of CRC cells in combination with cetuximab, a monoclonal antibody against EGFR. Multivariate analysis indicated that low *miR-7* expression was an independent prognostic factor for poor survival ($P = 0.0430$). *In vitro* assays showed that EGFR and RAF-1 are direct targets of *miR-7*, which potently suppressed the proliferation of CRC cells, and, interestingly, that the growth inhibitory effect of each of these was enhanced by cetuximab. *miR-7* is a meaningful prognostic marker. Furthermore, these data indicate that *miR-7* precursor, alone or in combination with cetuximab, may be useful in therapy against CRC.

Introduction

Over 1.2 million new cases of colorectal cancer (CRC) are diagnosed worldwide every year, and CRC accounts for 8% of cancer deaths (1). In recent years, the incidence of CRC and associated mortality have dramatically increased in Japan (2). According to the 2008 edition of Global Cancer Facts & Figures, CRC is globally the third and fourth most common cause of death from a malignant neoplasm among women and men, respectively. Surgery and administration of anticancer drugs, such as oxaliplatin, have been the conventional treatments for CRC. Recently, targeted molecular treatments using antibodies, such as anti-vascular endothelial growth factor (*VEGF*) antibody and anti-epidermal growth factor receptor (EGFR) antibody, have also been employed. Colon cancer chemotherapy can therefore involve traditional anticancer agents, which have non-specific cytotoxic effects, and/or agents that target specific molecules and block specific intracellular signaling pathways, with both approaches playing an important role in improving prognosis and extending the lifespans of patients (3–6).

The EGF receptor, which is a member of the ErbB receptor family, regulates important processes, such as cell proliferation, differentiation and development (7–10). It has been reported to be overexpressed in a variety of solid tumors,

Received: September 4, 2013; Revised: October 10, 2014; Accepted: October 18, 2014